Photoluminescence of Platinum(II) Complexes with Diazine-Based Ligands

Mariia Hruzd, Raphaël Durand, Sébastien Gauthier, Pascal Le Poul, Françoise Robin-Le Guen, Sylvain Achelle

Review

doi.org/10.1002/tcr.202300335
tcr.wiley-vch.de

THE CHEMICAL RECORD

Photoluminescence of Platinum(II) Complexes with Diazine-Based Ligands

Mariia Hruzd, Raphaël Durand, Sébastien Gauthier, Pascal le Poul, Françoise Robin-le Guen, and Sylvain Achelle*[a]

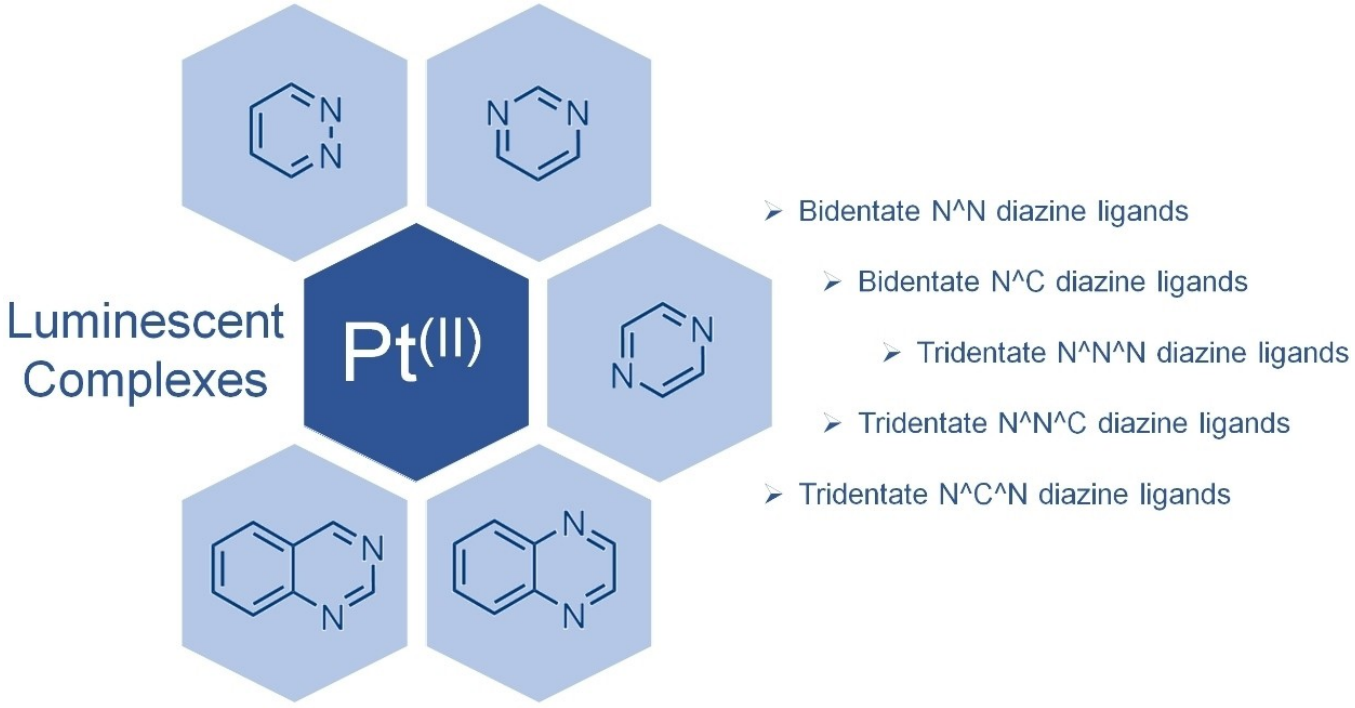

Abstract: In the last past twenty years, research on luminescent platinum (II) complexes has been intensively developed for useful application such as organic light emitting diodes (OLEDs). More recently, new photoluminescent complexes based on diazine ligands (pyrimidine, pyrazine, pyridazine, quinazoline and quinoxaline) have been developed in this context. This review will summarize the photophysical properties of most of the phosphorescent diazine Pt(II) complexes described in the literature and compare the results to pyridine analogues whenever possible. Based on the emission color, and the photoluminescence quantum yield (PLQY) values, the relationship between structure modification, and photophysical properties are highlighted. Tuning of emission color, quantum yields in solution and solid state and, for some complexes, aggregation induced emission (AIE) or thermally activated delayed fluorescence (TADF) properties are described. When emitting OLEDs have been built from diazine Pt(II) complexes, the external quantum efficiency (EQE) values and luminance for different emission wavelengths and in some cases, chromaticity coordinates obtained from devices, are given. Finally, this review highlights the growing interest in studies of new luminescent diazine Pt(II) complexes for OLED applications.

Keywords: platinum (II), phosphorescence, pyrimidine, OLEDs, cyclometalation

1. Introduction

Platinum has multiple oxidation states, ranging from zero to six, with +2 and +4 being the most common, particularly in coordination chemistry. The four-coordinate platinum(II) complexes with a d^8 electronic configuration exhibit a more or less distorted square-planar geometry depending on the ligands, the planar aspect being systematically observed. This geometry pushes a single unoccupied orbital to higher energies, compared to others ones, whilst allowing substantial stabilization of three of the occupied orbitals (Figure 1a).[1] Through axial interactions, such platinum systems can potentially offer reactivity not available to six-coordinate d^6 complexes due to their square-planar coordination geometry. Self-quenching, cross-quenching,[2] and photochemical reactivity[3] are all factors that make emissive Pt(II) complexes of particular interest. Many of the important features that define the absorption, luminescence, and other excited state characteristics of Pt(II) complexes are attributed to the square planar conformation.

Some photoluminescent Pt(II) complexes based on monodentate ligands (imidazolylidene…) have been synthesized, characterized and studied for their photophysical properties.[4] Nevertheless, due to the lack of planar geometry and rigidity of these complexes, the performance of the device and the purity of the colors are below the current state of the art of OLEDs in comparison to complexes bearing multidentate ligands, in particular cyclometalated ones. In Pt(II) complexes, the d-d excited state has a strong influence on the photophysical properties. Cyclometalating ligand, *ie* an organic ligand coordinated to metal center and forming at least one metal-carbon σ bond, increases the rigidity of the complex. Both the chelate effect and strong σ-donating ligand destabilize the dx2-y2 orbital and thus help to prevent population of the "dark" metal-centered (MC) excited states. Moreover, the synergic effect of the strong σ-donating Pt–C bond and the π-accepting character of the heterocycle, leads to stabilization of the metal to ligand charge transfer (MLCT) states.[5] In this way, under the influence of cyclometalation, the energy of the ^{3}MLCT is reduced and at the same time, the energy of MC level is increased, ΔE is therefore increased and non-radiative decay is inhibited (Figure 1b).[6] Moreover, the rigidity due to cyclometalation reduces the structural distortion of the Pt(II) complexes that leads to lower k_{nr} by decreasing the value of vibronic coupling constant between the T_1 and S_0 states called the Huang–Rhys factor.[7] It should be noted that the ligand-centred (LC, also called π-π*) states are extremely important and today it is established that mixtures of MLCT and LC (sometimes including ligand to metal charge transfer (LMCT) and and ligand to ligand charge transfer (LLCT)) contributions are beneficial for the absorption intensity and luminescence quantum yields and play a role in color emission.[8] Moreover, it has been reported that complexes containing chelate ligands NN′ and NCN′ exhibit more complex excited states then their symmetric NN and NCN analogues.[8c] Pt(II) complexes can also exhibit metal-metal-to-ligand charge transfer (MMLCT) excited state due to metallophilic interactions,

[a] *M. Hruzd, R. Durand, S. Gauthier, P. le Poul, F. Robin-le Guen, S. Achelle*
Univ Rennes, CNRS, Institut des Sciences Chimiques de Rennes – UMR 6226, 5000 Rennes, France
E-mail: sylvain.achelle@univ-rennes1.fr

Mariia HRUZD earned her bachelor's degree from the Taras Shevchenko National University of Kyiv (KNU), Ukraine. She then pursued a double master's degree at KNU and at the University of Angers, France. In 2019 Mariia secured a Ph.D. position at the University of Rennes1, France, under the guidance of Prof. Françoise Robin-le Guen, Dr. Sylvain Achelle and Dr. Sébastien Gauthier. Various series of new cyclometalated organometallic complexes with tunable photophysical and electrochemical properties were developed. She is currently a Post-Doctoral researcher at the University of Strasbourg, France, and is working on reductive chemical recycling of polyurethanes using organometallic complexes.

Raphaël Durand studied organic chemistry at the Ecole Nationale Supérieure de Chimie de Rennes and received his Ph.D. in organometallic chemistry in 2018 from the Université de Rennes (France) under the supervision of Françoise Robin-Le Guen, Sylvain Achelle et Sébastien Gauthier. He moved then to Mulhouse (France) in the Laboratoire d'Innovation Moléculaire et Applications to study enzymatic biomimetism. After this one-year post-doctoral experience at the border between organic chemistry and biology, he returned to Bretagne to become an guest researcher in the Institut des Sciences Chimiques de Rennes. His main research topics are focused on the design of π-conjugated heterocyclic and organometallic systems, especially for nonlinear optics

Sébastien Gauthier obtained his Ph.D. in organometallic chemistry in 2006 under the direction of Pr. Kay Severin at the Swiss Federal Institute of Technology in Lausanne (Switzerland). In 2010, after three post-doctoral stays at the Swiss Federal Institute of Technology in Zurich (Switzerland), Texas A&M University (USA) and Ecole Nationale Supérieure de Chimie de Paris (France), he took up the position of associate professor at the Université de Rennes 1 (IUT de Lannion) and joins the Heterocyclic Organometallics group at the Institut des Sciences Chimiques de Rennes. In 2020, he obtained the habilitation to direct research. His research mainly revolves around the development of various π-conjugated heterocyclic push-pull organic and organometallic molecular systems, exhibiting properties, and performances for Dye-Sensitized Solar Cells (DSSCs), Non-Linear Optics (NLO) and Organic Light Emitting Diodes (OLED) applications.

Pascal Le Poul was recruited as associate professor at IUT Lannion, University of Rennes in 2005 after his Ph.D. received in 1999 from University of Rennes. His research topics include the development of heterocyclic organometallic derivatives based on pyrylium cations and methylenepyran moieties for Non-Linear Optics, Dye-Sensitized Solar Cells and luminescence. He has published 33 articles in international journals.

Françoise Robin-le Guen received her Ph.D. in organometallic chemistry from the University of Bretagne Occidentale (Brest, France). She is currently full professor at IUT Lannion, University of Rennes and head of the heterocyclic organometallic teams at the Chemical Sciences Institute of Rennes. Her main research topics are focused on the design of π-conjugated heterocyclic and organometallic systems for dye-sensitized solar cells, luminescence and nonlinear optics.

Sylvain Achelle received his Ph.D. in organic chemistry in 2007 from INSA Rouen (France). After two post-doctoral stays at the Universidad de Castilla-La Mancha (Spain) and Institut Curie (France), he was recruited as associate professor at IUT Lannion, University of Rennes, in 2010. He obtained the habilitation to direct research in 2014. His main research topics include the luminescence and nonlinear optical properties of organic and organometallic heterocyclic derivatives. He has published 89 scientific articles (h-index: 33 according to the Web of Science) and he is currently associate editor of the journal Dyes & Pigments.

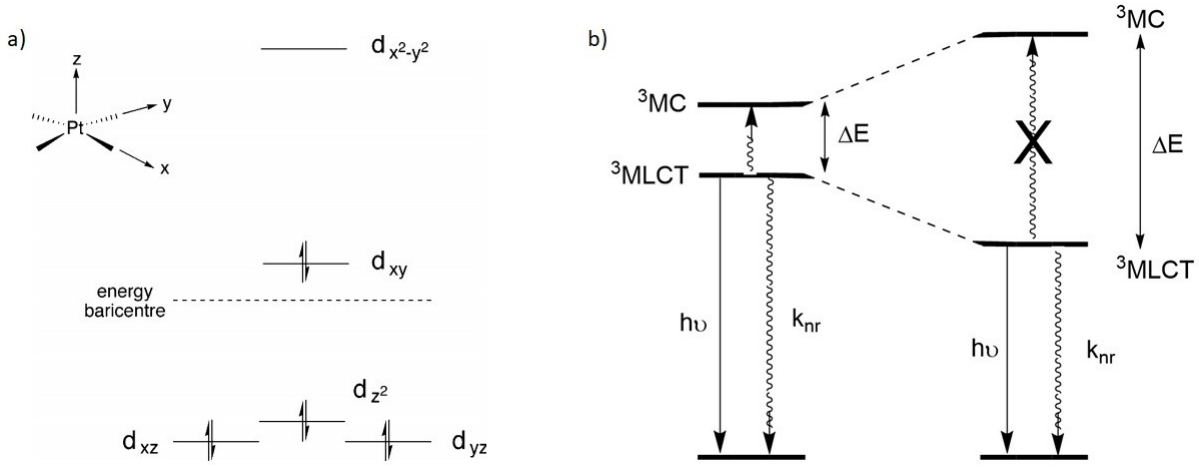

Figure 1. a) Simple ligand field-splitting diagram for metal d orbitals in a square planar complex; b) Schematic illustration of the influence of cyclometallation on the energies of MLCT and MC states. Reproduced from Ref. [6] with permission from Royal Society of Chemistry.

leading to unique near infrared luminescence that is highly sensitive to environmental factors.[9]

The design of cyclometalating ligand is mainly focused on improving the luminescent quantum efficiency and tuning the color of the emission color. The impacts of the cyclometalating ligand relate to the rigidity of the complex, the ligand field strength as well as the HOMO and LUMO levels which must be managed to allow for the participation of the heavy platinum atom in the emissive transition state. In this context, cyclometalated Pt(II) complexes have been extensively used for their phosphorescent properties and have found application in second generation organic light emitting diodes (OLEDs).[10] Many cyclometalating ligands represent combinations of pyridyl and phenyl moieties or derivatives thereof thus allowing to generate bidentate CN, tridentate CNN, NCN, or CNC, as well as tetradentate ligands of variable composition.[11]

The diazines are six-membered heterocycles with two nitrogen atoms. There are three isomers depending on the arrangement of the nitrogen atoms: pyridazine (1,2-diazine), pyrimidine (1,3-diazine) and pyrazine (1,4-diazine), quinazoline and quinoxaline corresponding respectively to benzopyrimidine and benzopyrazine (Figure 2). Diazines are an important class of ligands in coordination,[12] supramolecular,[13] and bioinorganic chemistry.[14] The pyrimidine system is also an important pharmacophore.[15] The diazine rings exhibit a π-deficient character and have been extensively used as electron-withdrawing part in push-pull structures with a large range of applications (fluorescent sensors, photovoltaic cells, nonlinear optical materials, Etc).[16] Diazine based ligands are strong π-electron acceptors which are able to accept electron density from metal centers in metal-ligand back-bonding.[17] The π-accepting properties calculated

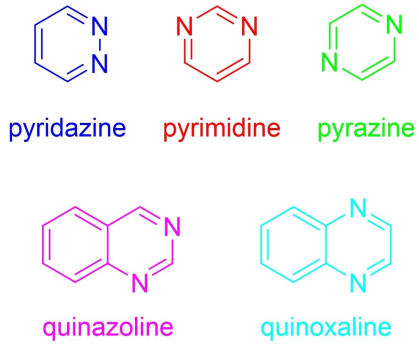

Figure 2. Structure of diazine and benzodiazine heterocycles.

through the difference in the total π-deficiency (TOTπD) of the heteroaromatic system are increased in the following order: pyridine (0.21) < pyrazine (0.28) < pyrimidine (0.42).[18] These fragments have attracted much attention due to their versatility and strong coordinating ability with a wide range of metal ions.[19] Besides, due to the presence of two nitrogen lone pairs, diazines have the ability to coordinate to two similar or different metal centers simultaneously. Consequently, the two nitrogen-based ligands afforded a number of interesting structures comprising coordination polymers,[20] and mononuclear to polynuclear coordination metal complexes.[21] Among diazine-based ligands, ligands with pyrimidine fragments are the most used. This fragment can be easily substituted in position 2 and 4 to form bidentate and tridentate ligands.[22] All these advantages make pyrimidine a highly attractive building block for the construction of coordination complexes with bi-, tri- or tetradentate ligands. Pyrimidine has a lower un-occupied molecular orbital (LUMO) than pyridine, which leads to modification of charge

transfer energy and therefore photophysical properties (Figure 3).[23]

In this contribution we will summarize the various examples of photoluminescent Pt(II) complexes with diazine-based ligands. This review will be mainly focused on cyclometalating ligands but will also include few examples of complexes bearing diazine-based NN and NNN ligands. Complexes are classified by their coordination pattern: namely NN, NC, NNN, NCN and NNC ligands. Whenever possible, comparison with pyridine analogue complexes will be carried out and structure-property relationships will be highlighted.

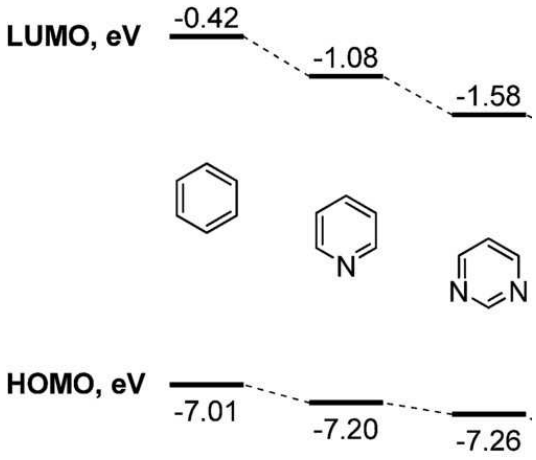

Figure 3. Calculated HOMO and LUMO energy levels of six-membered aryl cycles of benzene, pyridine and pyrimidine Gaussian03 W, B3LYP, 6-31 + G(d,p)). Reproduced from Ref. [23] with permission from Royal Society of Chemistry.

2. Complexes with Bidentate NN Diazine-Based Ligands

Platinum(II) complexes with bidentate diimine (NN) ligands have attracted worldwide attention over the past few decades, with numerous reports and investigations into their unique features.[24] The nature of the emissive states of bidentate NN Pt(II) complexes can be easily tuned by introducing different ancillary ligands. Moreover, the incorporation of strong-field ligands into the platinum(II) metal center can enhances the emission efficiency by raising the nonradiative d-d state to a higher energy level, thus making it thermally less accessible. Examples of bidentate NN Pt(II) complexes containing diazine-based ligands are limited in the literature.

Few Pt(II) complexes based on NN pyridylpyridazine ligands have been described in the literature as catalysts but their luminescence properties were not described.[25]

A series of functional pyrimidinyl-, pyridinyl-, and pyrazinyl pyrazolate Pt(II) complexes **1**–**8** has been designed (Figure 4).[26,27,28] These complexes all have a strong tendency to form aggregates in solid-state, leading to the appearance of low-lying MMLCT excited states (main character of the excited state). They are highly emissive in vacuum deposited thin film with emission ranging from 542 to 740 nm (Table 1). The nature of the azine has a direct impact on the Pt···Pt interactions, which leads to the emission tuning. Red shift of emission is observed in the following order pyrimidin-

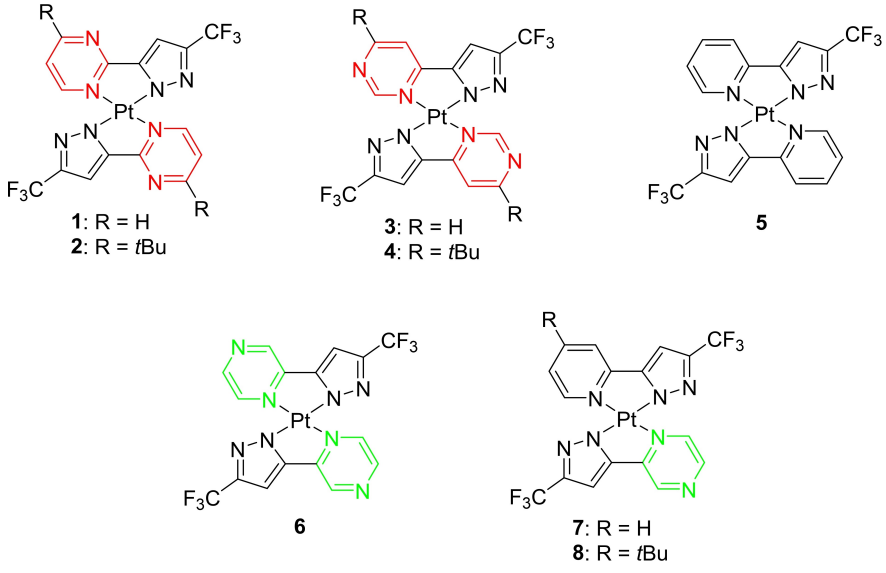

Figure 4. Structure of complexes **1**–**8** with NN ligands.

Table 1. Photophysical properties of Pt(II) complexes **1–8** as vacuum deposited thin film.

Pt(II) complex	Absorption λ_{max} (nm) ($\varepsilon \times 10^{-3}$ M^{-1} cm^{-1})[a]	Emission λ_{max} (nm)	PLQY (%)	τ (ns)[b]	Ref.
1	267 (40.1), 400 (15.6)	542	75	486	[26]
2	266 (44.3), 474 (14.9)	603	86	327	[26]
3	262 (65.8), 501 (20.6)	654	78	273	[26]
4	241 (40.9), 512 (16.2)	662	61	240	[26]
5	256 (24), 310 (19,7), 330 (12,3), 377 (2,9), 389 (2,5)	595	24	300	[27c]
6	330 (13), 387 (2.3)	740	81	313	[28]
7	322 (14.2), 397 (2.2)	703	55	365	[28]
8	328 (13.1), 385 (2.7)	673	82	309	[28]

[a] Measured in degassed THF solution for complexes **6–8**; [b] Measured on sublimed powder sample for complexes **6–8**.

2-yl (**1**) < pyridin-2-yl (**5**) < pyrimidin-4-yl (**3**) < pyrazin-2-yl (**6**). In the latest one, the replacement of one of the two pyrazine fragments by a pyridine one (complexes **7** and **8**) induces a blue-shift of emission in the pyrimidinyl series. Surprisingly, the *tert*-butyl bulky substituent strengthens the intermolecular Pt···Pt unbonding interaction, resulting in a red-shifted emission observed for the complexes **2** and **4** *vs* **1** and **3** respectively. The opposite effect was expected due to the steric hindrance of the *tert*-butyl group, which prevents the Pt···Pt formation.[29] However, the expected trend is observed in the pyrazinyl series with blue shifted emission for **8**, *tert*-butyl analogue of **7**.

Non-doped OLED devices have been fabricated with external quantum efficiency (EQE) up to 27.5 % at 10^3 cd m^{-2} with $CIE_{x,y}$ of (0.56, 0.44) using complex **2** as emitter. On the other hand, complex **6** permitted the fabrication of NIR-OLED with EQE of 24 %, one of the highest EQE reported so far. This high device performances can be attributed to the high PLQY as well as horizontal orientation of the emission dipoles.

3. Cyclometalated Complexes with Bidentate NC Diazine-Based Ligands

In order to improve luminescence properties of bidentate Pt(II) complexes and to enhance electroluminescent performance of their OLED devices, cyclometalating bidentate ligands can be incorporated into the platinum(II) metal center.[30] As mentioned earlier, the anionic carbon atom acting as a strong σ-donor can raise the energy of the non-radiative d-d excited state, diminishing its competitiveness compared to other emissive states and thereby promoting the luminescence of complexes. In addition, the enhanced stability of bidentate cyclometalated NC Pt(II) complexes, arising from metal-carbon bonding, improves their processability for OLED applications. This chapter introduces bidentate NC Pt(II) complexes with ligands incorporating the different diazine rings.

3.1. Pyridazine Based Ligands

Zhukovsky and coworkers have designed a series of bis Pt(II) complexes **9–15** based on 3,6-diphenylpyridazine ligands (Figure 5).[31] Depending on the nature of ancillary ligands the complexes are either anionic (**9–11**, with chloride ancillary ligands) or cationic (**12–15**, with phosphine ancillary ligands). The pyridazine ring enables the complexation of two platinum atoms with bridging chloride ligands. Both cationic and anionic complexes exhibit weak orange phosphorescence with PLQY below 3.4 % in degassed solution (Table 2). The nature of the lowest excited state for complexes **9–15** is a mixture of intraligand (IL) and MLCT with dominance of IL for anionic complexes (**9–11**) and MLCT for cationic ones (**12–15**) without significant modification of emission energy. The replacement of phenyl substituents by thien-2-yl ones (complexes **16** and **17**) induces a significant red shift (> 100 nm) of emission bands, along with a change in the nature of the excited state.[32] TD-DFT calculations indicate that the emission originates mainly from LLCT with MLCT and LC contributions.

3.2. Pyrimidine Based Ligands

Complexes with pyrimidine, especially 2-phenylpyrimidine ligand, are much more common in the literature. Sun and coworkers have designed complex **18** based on 2-(4-*N*,*N*-diphenylaminophenyl)pyrimidine ligand and acetylacetonate-(Acac) ancillary ligand (Figure 6).[33] This molecule exhibits weak phosphorescence in THF but shows strong aggregation-inducted emission (AIE) in mixture of THF and water when the water ratio is higher than 70 %. In pure THF, emission was attributed to ILCT. The emission enhancement upon addition of water is attributed to MMLCT transition induced by the molecular aggregation. The 6 wt % doped device based on complex **18** displays green-yellow emission with a peak EQE of 9.2 %. Complex **18** has also been used in nondoped OLED that exhibits NIR emission with EQE up to 9.8 %, which corresponds to significantly higher performance than

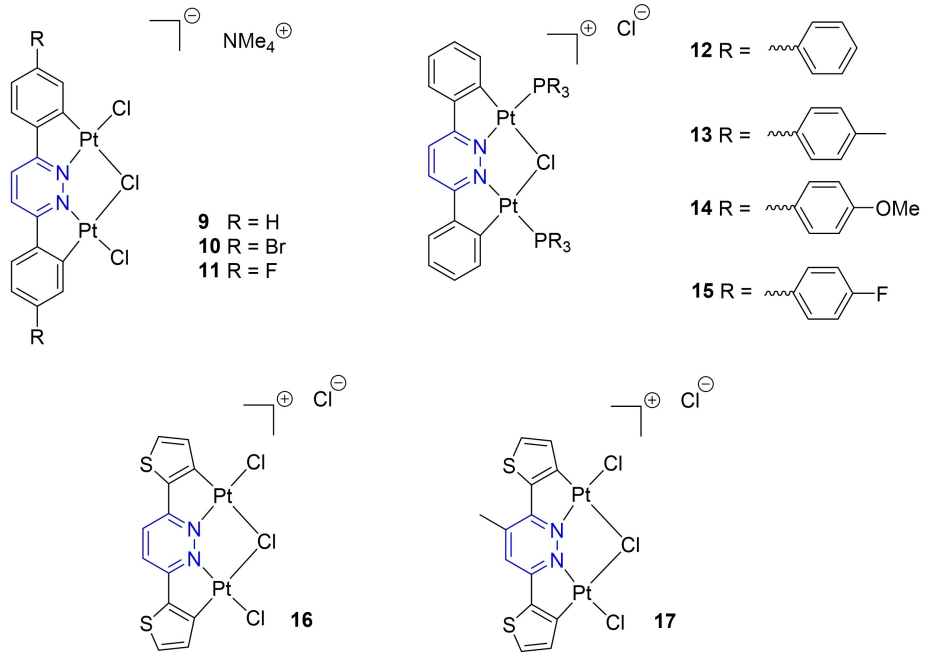

Figure 5. Structure of cyclometalated complexes **9**–**17** with NC ligands containing pyridazine fragment.

Table 2. Photophysical properties of Pt(II) complexes **9**–**17** in degassed acetone solution at room temperature (RT).

Pt(II) complex	Absorption λ_{max} (nm) ($\varepsilon \times 10^{-3}$ $M^{-1}cm^{-1}$)	Emission λ_{max} (nm)	PLQY (%)	τ (ns)	Ref.
9	398 (18.0)	595, 632[b]	3.4	190	[31]
10	395 (22.0)	591, 625[b]	1.0	140	[31]
11	388 (13.5)	584, 624[b]	1.7	220	[31]
12a	261 (36.2), 332 (18.0), 379 (15.1)	575sh, 612	2.3	310	[31]
13a	261sh (48.7), 321 (25.7), 375 (15.7)	620	1.8	250	[31]
14a	252 (69.8), 328 (16.2), 381 (13.4)	580sh, 614	1.2	130	[31]
15a	262 (33.1), 331 (17.8), 378 (14.0)	573sh, 613	2.9	160	[31]
16	408 (22.2), 478 (4.5), 510sh (2.7)	693, 751, 840sh	2.7	2700	[32]
17	401 (17.7), 468 (3.9)	681, 739, 830sh	3.3	3300	[32]

[a] in DCM, [b] Vibronic structure with 980–1080 cm^{-1} spacing.

the pyridine analog **18a** (EQE up to 8.5%).[34] Zhao and coworkers have designed similar complex **19** with pyridine and chloride ancillary ligands (Figure 6).[35] Under excitation at 360 nm, this complex exhibits emission at 478 and 540 nm with low PLQY (1%). These photophysical data are similar to the pyridine analogue **19a** (Table 3). The high energy band corresponds to fluorescence and is attributed to ligand centered excited state while the band at 540 nm corresponds to phosphorescence according to emission lifetime. It should be noted that the fluorescence emission is much weaker than that of pyridine analogue **19a**. An OLED device with the following structure: ITO/PEDOT:PSS (45 nm)/**19** 8% Pt:CBP (40 nm)/TPBi (45 nm)/LiF:Al (1:100 nm) was fabricated and exhibits attractive characteristics (L_{max} of 6801 cd m^{-2} at 14.4 V, a η_L of 53.8 cd A^{-1}, a EQE of 14.8% and a η_P of 45.2 lm W^{-1}), slightly lower than the phenylpyridine based analogue complex **19a**. Based on this model complex, Fecková and coworkers have designed complexes **20**–**23** and **25** bearing electron-donating (EDG) or electron-withdrawing (EWG) groups on the phenyl ring in *para* position related to either the pyrimidine (complex **21**) or the platinum atoms (complexes **22**, **23** and **25**, Figure 6).[36] In DCM solution, it appears that only complexes **23** and **25** with EDG in *para* position to the Pt atoms are luminescent in degassed DCM with a bathochromic shift of emission with increasing strength of EDG (**23** (OMe):570 nm, **25** (NPh_2):628 nm, with PLQY up to 40% for **23** (Table 3). The whole series of complexes exhibits nevertheless strong emission in solid state from green to red

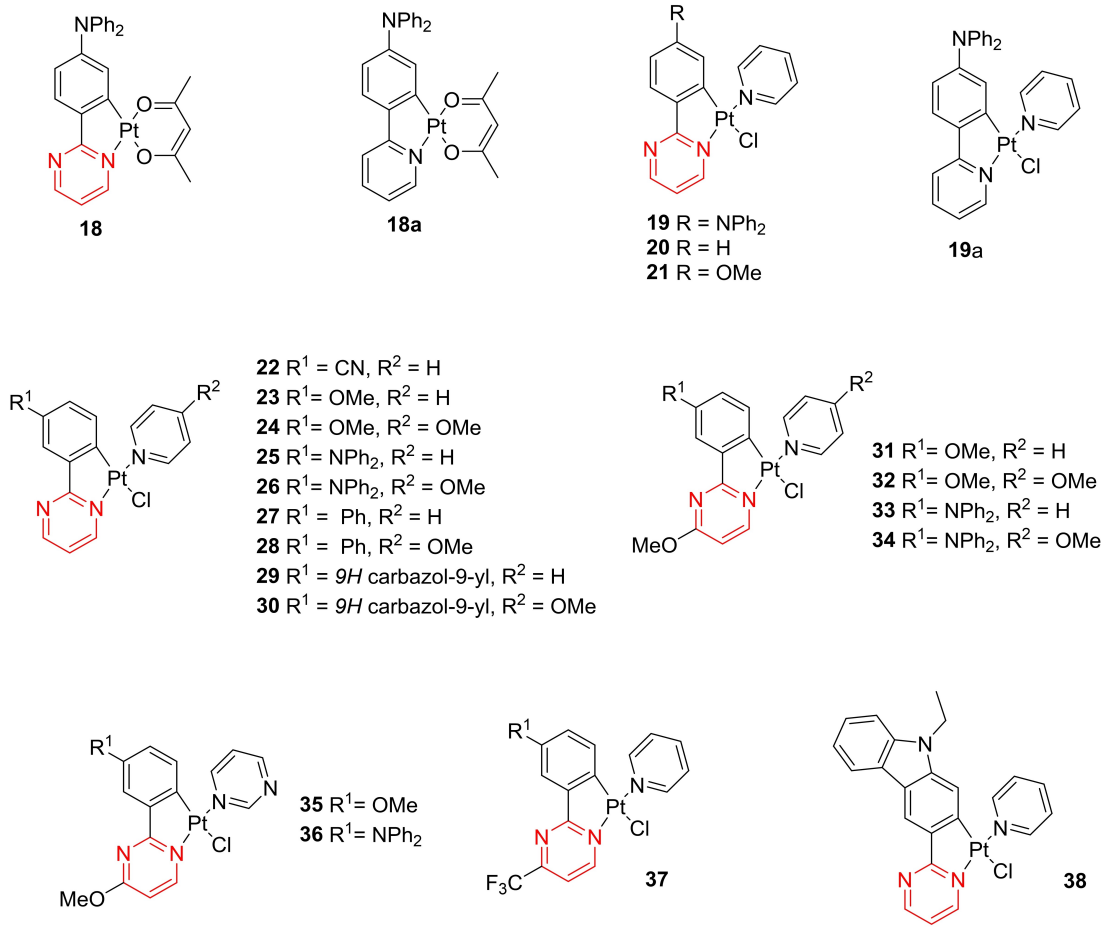

Figure 6. Structure of cyclometalated complexes **18**–**38** with NC ligands containing pyrimidine and their pyridine analogues **18a** and **19a**.

region of the spectrum, depending on the substituents. Other structural modifications such as the introduction of different donor groups on the Phenyl ring in the *para* position to the Pt atoms, the use of different ancillary ligands and the introduction of –OMe or $–CF_3$ substituents into the pyrimidine ring were performed and the complexes **24** and **26**–**38** were prepared (Figure 6).[37] The following structure properties relationships can be highlighted: the strength of the EDG on the phenyl ring tunes emission wavelength by modification of HOMO energy level: the stronger the EDG, the more bathochromically shifted the emission (Figure 7). Emission wavelength can be modulated by introducing a methoxy EDG (hypsochromic shift) or a trifluoromethyl EWG (bathochromic shift) at the C4 position of the pyrimidine ring tuning the LUMO energy level. The trifluoromethyl group in the structure of complex **37** significantly decreases PLQY. The ancillary ligand has a moderate influence on emission position but plays a significant role on PLQY, the 4-methoxypyridine ligand has a beneficial

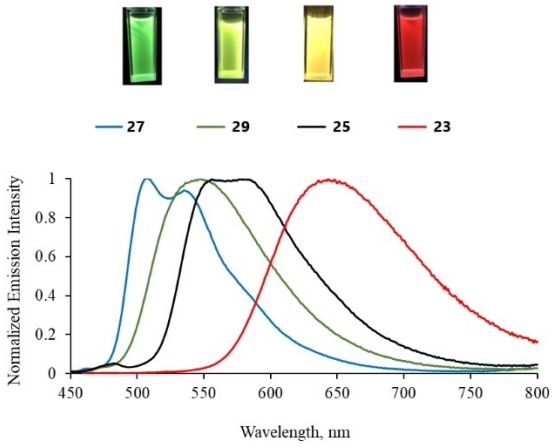

Figure 7. Normalized emission spectra of phenylpyrimidine complexes **23**, **25**, **27** and **29**. Reproduced from Ref. [37] with permission from Royal Society of Chemistry.

Table 3. Photophysical properties of Pt(II) complexes **19**–**38** in degassed DCM solution at RT.

Pt(II) complex	Absorption λ_{max} (nm) ($\varepsilon \times 10^{-3}$ M^{-1} cm^{-1})	Emission λ_{max} (nm)	PLQY (%)	τ (ns)	Ref.
19	303 (31.6), 338 (27.5), 371 (35.5), 424 (37.1)	481, 548, 588sh	1	229[a]	[35]
19a	311 (36.3), 338 (37.1), 370 (35.4), 425 (31.6)	478, 540, 587sh	3	271[b]	[35]
20	286sh (13.9), 338 (6.1), 386 (2.0)	_[c]	_[c]	_[c]	[36]
21	264 (24.1), 314 (14.2), 384 (1.8)	_[c]	_[c]	_[c]	[36]
22	270 (36.2), 335 (4.5), 382 (2.1)	_[c]	_[c]	_[c]	[36]
23	283sh (14.7), 346 (5.5), 414 (2.6)	570	40	12600	[36]
24	289 (13.9), 351 (5.55), 430 (2.55)	556, 582	54	9700	[37]
25	285 (27.0), 292 (35.2), 438 (2.3)	628	5	8860	[36]
26	289 (13.9), 351 (5.55), 430 (2.55)	556, 582	54	9700	[37]
27	293 (50.), 350 (8.24), 433 (2.17)	630	6	6100	[37]
28	277 (41.3), 346 (3.94), 404 (1.27)	508, 538	5	8500	[37]
29	291 (38.7), 341 (10.6), 412 (2.29)	574	12	4700	[37]
30	270 (36.4), 330 (9.11), 342 (10.0), 415 (2.46)	543	15	3900	[37]
31	297 (10.8), 341 (2.89), 416 (4.57)	545, 575	47	12000	[37]
32	288 (18.4), 338 (5.04), 415 (2.99)	545, 575	15	7700	[37]
33	293 (38.5), 350 (5.71), 437 (1.67)	630	8	6800	[37]
34	293 (50.0), 350 (8.24), 433 (2.17)	630	6	6100	[37]
35	285 (14.3), 345 (4.69), 413 (2.49)	543, 571	9	4300	[37]
36	292 (28.7), 342 (6.53), 442 (1.74)	630	3	6000	[37]
37	299 (44.4), 345 (3.57), 383 (1.45), 477 (0.84)	642	<1	_[c]	[37]
38	271 (26.7), 298 (12.0), 341 (14.1), 379 (8.33), 455 (1.84)	583	22	7300	[37]

[a] at 548 nm, [b] at 540 nm [c]emission too low to permit accurate measurement.

effect, particularly in solid state. Complexes **23** and **30** exhibit the highest PLQY in solid state (respectively 20 and 14%). Complex **38** with the *9H*-carbazol-2-yl-pyrimidine NC ligand shows yellow-orange emission with a PLQY of 22%.

Damm and coworkers have designed the metallogens **39**–**44** (Figure 8).[38] These complexes show luminescence in DCM but no relation between length and number of alkyl chains and position/intensity of emission bands was found. Complexes **40**, **41** and **43** exhibit one emission band below 440 nm whereas complexes **39**, **42** and **44** exhibit an additional emission band above 490 nm attributed to intermolecular Pt···Pt interaction.

The presence of two nitrogen atoms in the structure of the pyrimidine ring allows the complexation of two Pt(II) atoms. In this context, the complexes **46** and **48**–**50** were designed (Figure 9).[39,40,41,42] As shown when comparing complexes **45**, **47** *vs* **46** and **48** respectively, the introduction of a second Pt(II) atom induces a red shift of absorption and emission in solution as well as an increase of PLQY (Table 4). When comparing complex **46** (phenyl-based) and **49** (thien-2-yl-based), a red shift of the emission is observed, accompanied by a decrease in the radiative constant kr (330 000 and 71 000 s^{-1}, respectively). However, the kr value of complex **49** is 4 times higher than that of related monometallic complexes.[41] The use of dithienyl groups instead of thienyl one in the structure of **50** induces also a red shift of emission in NIR with almost no emission of visible light <700 nm (Figure 10). For this compound, the T_1 state, the most relevant to phosphorescence, exhibits a LC character dominating over MLCT. This complex was employed in the design of solution-processed OLEDs,

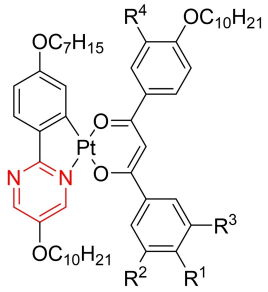

39 $R^1 = OC_{10}H_{21}$, $R^2 = R^3 = R^4 = H$
40 $R^1 = R^2 = OC_{10}H_{21}$, $R^3 = R^4 = H$
41 $R^1 = R^2 = R^4 = OC_{10}H_{21}$, $R^3 = H$
42 $R^1 = R^2 = R^3 = OC_{10}H_{21}$, $R^4 = H$
43 $R^1 = R^2 = R^3 = R^4 = OC_{10}H_{21}$
44 $R^1 = R^2 = R^3 = OC_6H_{13}$, $R^4 = OC_{10}H_{21}$

Figure 8. Structure of metallogens **39**–**44** with NC ligands containing pyrimidine unit.

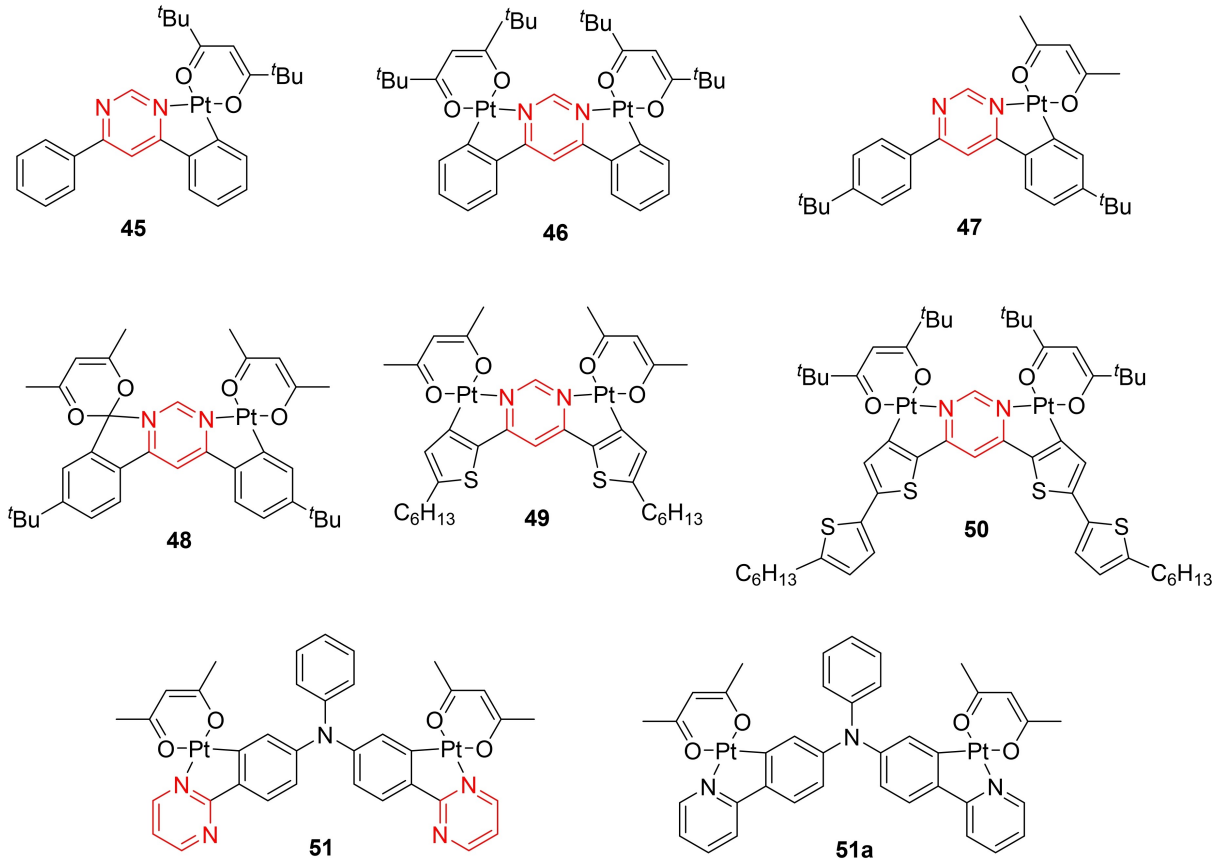

Figure 9. Structure of cyclometalated complexes **45**, **47**, bis-platinum derivatives **46** and **48**–**51** with NC ligands containing pyrimidine unit and pyridine analogue **51 a**.

Table 4. Photophysical properties of Pt(II) complexes **45**–**51** in degassed DCM solution at RT.

Pt(II) complex	Absorption λ_{max} (nm) ($\varepsilon \times 10^{-3}$ M^{-1} cm^{-1})	Emission λ_{max} (nm)	PLQY (%)	τ (ns)	Ref.
45	301 (31.6), 338sh (10.6), 408 (9.55)	521	25	1600	[39]
46	326 (63.2), 430 (17.1), 481 (24.3), 532sh (1.99)	558, 594	36	1100	[39]
47	308 (38.1), 338sh (18.5), 399 (11.9)	513, 536sh	31	2100	[40]
48	333 (47.2), 396 (12.2), 417 (16.6), 474 (24.5), 530 (1.43)	550, 591, 647	54	1700	[40]
49	347 (37.6), 400 (18.7), 470 (22.4), 500 (53.8)	610, 660sh	85	12000	[41]
50 a	382 (40.9), 421 (31.5), 562 (84.1)	725, 805	17	9000	[42]
51	356 (11.7), 451 (16.2)	492, 554	12	180	[43]
51 a	336 (11.8), 444 (14.8)	492, 552	11	130	[43]

[a] in toluene.

resulting in an EQE of 3.6%. Complex **51** is also a dinuclear complex but it is based two phenyl-pyrimidine units combined in a triphenylamine moiety, the two Pt(II) atoms are not complexed on the same pyrimidine ring (Figure 9).[43] This complex exhibits similar phosphorescence properties than pyridine analogue **51 a** with slightly higher k_r (5.33×10^5 s^{-1} *vs* 4.46×10^5 s^{-1} value and lower k_{nr} (50.2×10^5 s^{-1} *vs* 72.5×10^5 s^{-1}) value. It is stated that phosphorescence held in both cases LC character with a little LMCT feature. It should be noted that the dual emission observed with complexes **51** and **51a** corresponds to fluorescence (high energy band) and phosphorescence (low energy band). This phenomenon is attributed to the presence of the triphenylamine core, which reduces the contribution from the Pt center to HOMOs and weakens the spin-orbit interaction.

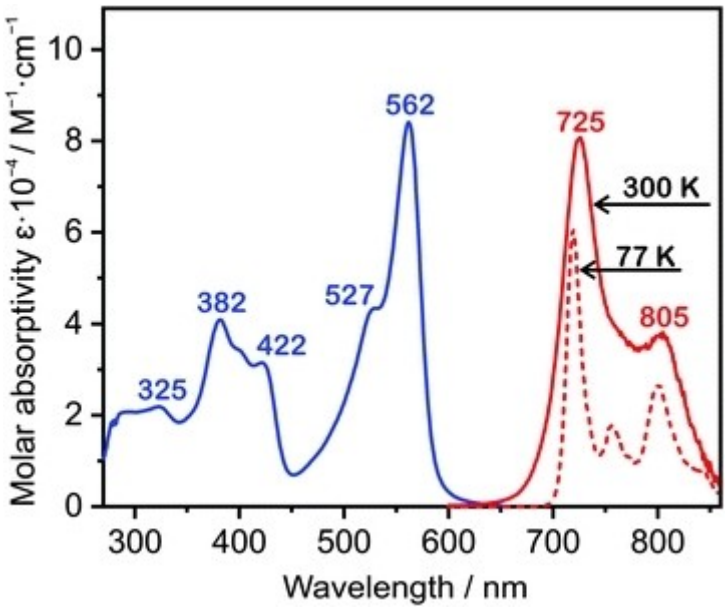

Figure 10. Absorption spectrum of **50** in toluene (10^{-5} M) at 300 K (blue line); emission spectrum under the same conditions (solid red line) and at 77 K (dashed red line), arbitrary intensity axis. Reproduced from Ref. [42] with permission from Royal Society of Chemistry.

Moreover, the pyrimidine has ability to form complexes not just with two similar metals but also with two different ones. Starting from 4,6-diphenylpyrimidine derivatives, Shafikov, Kozhevsnikov and coworkers have designed Ir(III)/Pt(II) complexes **52** and **53** (Figure 11).[40,44] Compared with **47**, the addition of Ir(III) metal center in the structure of complex **52** induces a red shifted emission (Table 5). For **52**, according to TD-DFT calculation, the triplet state T_1 can be assigned to a MLCT character involving the Ir(III) center and some less profound but still contributing spin orbit coupling at the Pt center. The presence of a second Pt(II) element in the structure of **53** induces an additional slight red shift of emission with a decrease of PLQY. Complex **52** was employed as the emissive guest compounds in host-guest light-emitting electrochemical cell that shows red emission ($\lambda_{peak} = 615$ nm) with EQE of 2.7 % at a luminance of 265 cd m^{-2}.

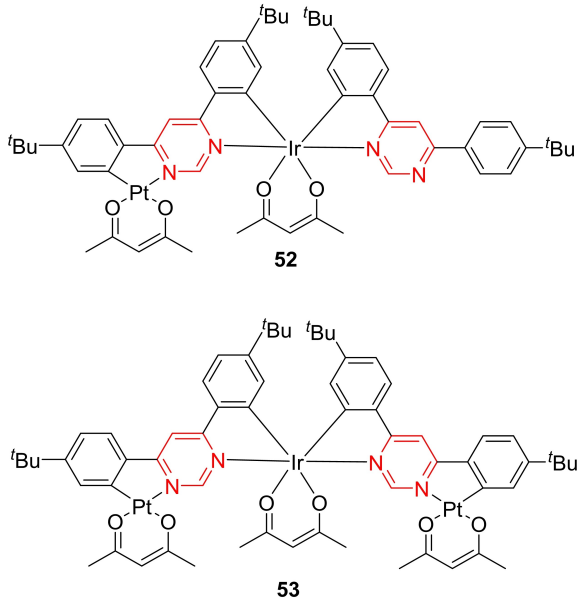

Figure 11. Structure of cyclometalated Ir(III)/Pt(II) complexes **52** and **53** with N^C ligands containing pyrimidine units.

Pt(II) complexes **54–66** with 5-(pyridin-2yl)pyrimidine type ligands have been described (Figure 12).[45,46,47] In these cases, the Pt(II) atom is linked to carbon atom of the pyrimidine ring. The PL spectra of complexes **54–57** in thin film exhibit NIR emission profile arising from an aggregated state (emission with ICT/MMLCT character) with PLQY > 20 % (Table 6). Pyrazinyl azolate ancillary ligands in the structure **55–57** induce red shifted emission due to a more stabilized LUMO orbital in comparison with pyridinyl azolate in the structure of complex **54**. Moreover, the enhanced π-accepting properties of pyrazinyl group strengthen the Pt–N bound and increase rigidity inducing higher emission efficiency. Complexes **55** and **56** were used to build non-doped NIR-emitting OLEDs with EQE of 10.61% at 794 nm and 9.58% at 803 nm respectively with low efficiency roll-off.[45] Due to the increased steric hindrance of 2,6-diisopropylphenyl fragment in the structure of complex **58**, intermolecular interactions are reduced. Contrary to complexes **54–57**, no obvious red-shifted absorption and emission are observed. The

Table 5. Photophysical properties of Ir(III)/Pt(II) complexes **52** and **53** in degassed DCM solution at RT.

Pt(II) complex	Absorption λ_{max} (nm) ($\varepsilon \times 10^{-3}$ M^{-1} cm^{-1})	Emission λ_{max} (nm)	PLQY (%)	τ (ns)	Ref.
52a	326 (59.9), 389 (21.6), 412 (20.0), 441 (17.8), 471 (17.0), 503 (8.8), 535 (9.1), 570 (8.0)	615	85	640	44
53	330 (69.7), 388 (24.5), 410 (24.8), 443 (24.4), 470 (26.3), 536 (11.4), 568 (13.1)	626	41	580	40

[a] in toluene.

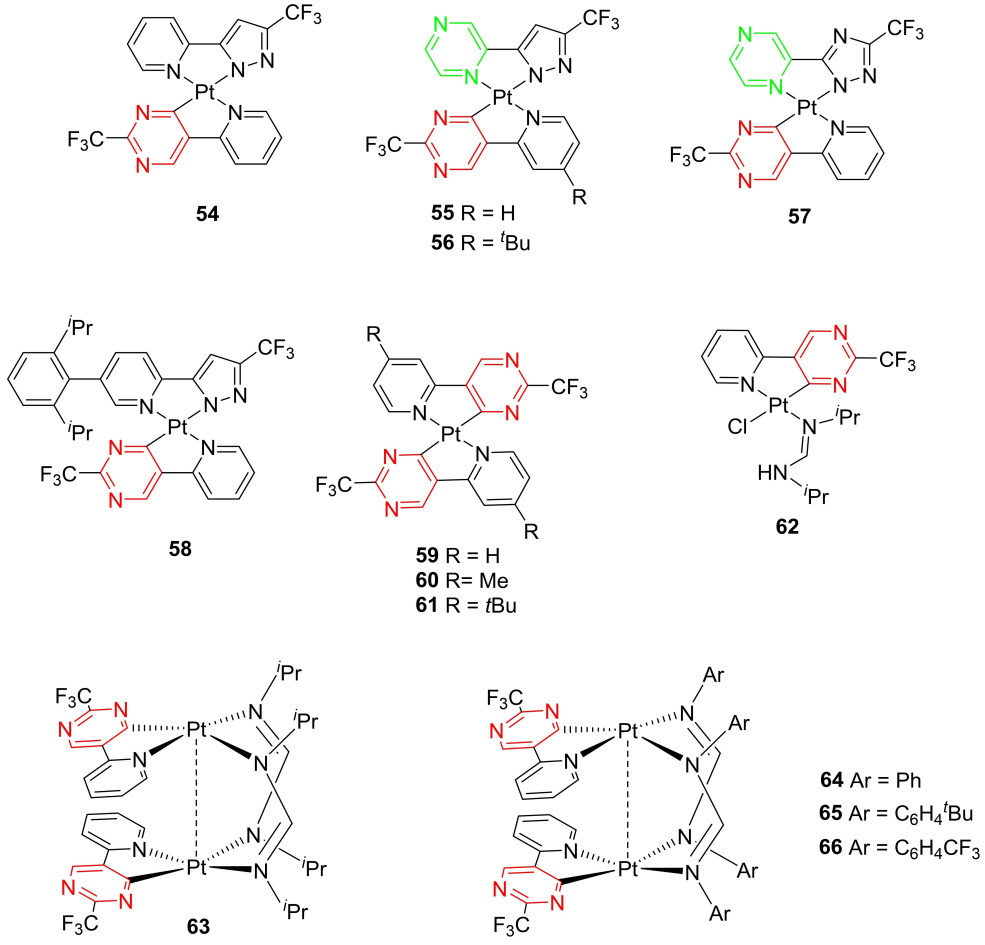

Figure 12. Complexes **54**–**66** with N^C 5-(pyridin-2-yl)pyrimidine ligands.

replacement of the pyrazol-5-yl fragment by a pyrimidin-4-yl one (**59** *vs* **54**), induced a significant red shift in emission up to 866 nm. Unlike the *cis*-cyclometalate observed in $[Pt(ppy)_2]$ (ppyH = 2-phenylpyridine) the complexes **59**–**61** show *trans*-configuration. This may be explained by the interligand C-H···N linkage between the two *trans*-oriented chelating ligands.[28c] In solid state, the complexes spontaneously self-assemble, and the associated excitonic coupling move the transition energy to deep red or NIR region (Table 6), with remarkable PLQY in the range of 5–12%. NIR OLEDs with an emission peak up to 930 nm, as observed in the case of complex **61**, were fabricated with EQE up to 2.14%.

Bis-platinum complexes **63**–**66** exhibit red-shifted emission compared to monoplatinum complex **62**. The structureless MMLCT emissions are due to intramolecular Pt···Pt interactions. For complexes **63**–**64**, PLQY are much higher in crystalline states than in thin films due to fewer defect in this morphology (PLQY up to 24% for **64**).

Table 6. Photophysical properties of Pt(II) complexes **54**–**66** as vacuum deposited thin film.

Pt(II) complex	Absorption λ_{max} (nm) ($\varepsilon \times 10^{-3}$ $M^{-1}cm^{-1}$)[a]	Emission λ_{max} (nm)	PLQY (%)	τ (ns)[b]	Ref.
54	570	776	20	540	[45]
55	582	832	38	520	[45]
56	573	820	28	710	[45]
57	548	802	24	790	[45]
58	400	608	40	5450	[45]
59	589	866	12	190	[46]
60	613	881	5.2	110	[46]
61	730	960	5.0	100	[46]
62	265 (21), 359 (4)	476, 511, 537	5.5	385	[47]
63	256 (42), 436 (3.5), 524 (.8)	732	< 1	26	[47]
64	262 (52), 325 (36), 417 (4.7), 528 (2.8)	758	< 1	41	[47]
65	263 (58), 321 (40), 428 (4.7), 530 (3.1)	769	< 1	31	[47]
66	271, (29), 331 (27), 519 (1.5)	726	< 1	84	[47]

[a] Measured in DCM solution for complexes **62**–**66**.

3.3. Pyrazine Based Ligands

Pt(II) complexes with pyrazine based NC ligand are rarer than pyrimidine analogues and only few are described in the literature (Figure 13).[37,39] When comparing complexes **67**–**70** with their pyrimidine counterparts (complexes **23**, **25**, **27**, **29**), a significant red shift of emission (~60 nm) is observed. It can be explained by the position of the second nitrogen atom in conjugated position *vs* the Pt(II) center in case of pyrazine (Tables 6 and 7). The really low emission intensity of complex **68** is attributed to a too strong charge transfer that disfavors the radiative return to ground state. For these complexes, excimer red-shifted emission is observed in solid state despite the presence of out of plane pyridine ancillary ligand. Red-shifted emission is also observed for complexes **72** with regards to pyridine and pyrimidine **72a** and **45** counterparts. The bathochromic shift is more pronounced in case of 2,5-diphenylpyrazine ligand (complex **71**) than with 2,3-diphenylpyrazine (complex **72**). As observed in the pyrimidine series, the complexation of a second Pt(II) center on 2,5-diphenylpyrazine (complex **73**) provokes a red-shifted emission with increased PLQY. This is less obvious for 2,3-diphenylpyrazine (complex **74**).

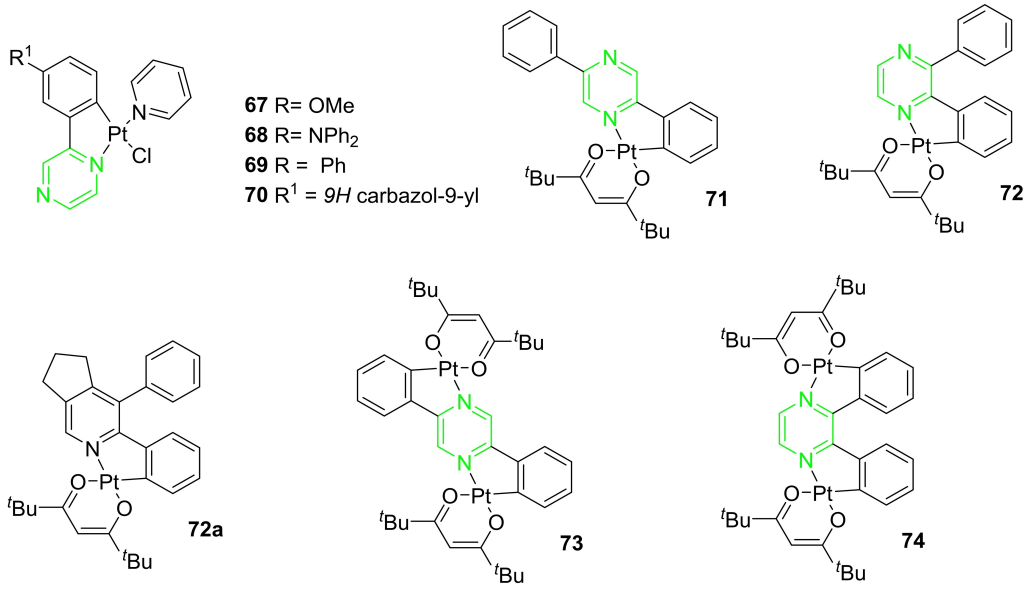

Figure 13. Cyclometalated complexes **67**–**74** with NC ligands containing pyrazine fragment and pyridine analogue **72a**.

Table 7. Photophysical properties of Pt(II) complexes **67**–**74** in degassed DCM solution at RT.

Pt(II) complex	Absorption λ_{max} (nm) ($\varepsilon\times10^{-3}$ M^{-1} cm^{-1})	Emission λ_{max} (nm)	PLQY (%)	τ (ns)	Ref.
67	319 (13.1), 357 (7.82), 466 (2.12)	630	12	6300	[37]
68	283 (60.0), 372 (4.31), 490 (1.57)	–[a]	–[a]	–[a]	[37]
69	321 (19.6), 347 (11.9), 445 (2.55)	583	30	7900	[37]
70	328 (13.2), 343 (10.6), 452 (1.02)	608	9	5600	[37]
71	299 (25.4), 342 (17.3), 398 (6.43), 435 (5.24)	565, 608	30	8900	[39]
72	292 (16.9), 340 (11.9), 398 (6.17), 449 (2.17)	554, 578	43	7700	[39]
72a	280 (18.2), 314 (8.5), 327 (8), 360 (5.8), 400sh (2.2)	490sh, 523	43	7400	[48]
73	296 (26.5), 333 (21.9), 372 (16.6), 453 (15.), 503 (6.83), 618 (0.34)	628, 685, 753	41	3200	[39]
74	301 (20.3), 319 (20.7), 390 (19.6), 451 (15.2), 572 (0.31)	612	37	4000	[39]

[a] Emission too low to permit accurate measurement.

3.4. Quinazoline Based Ligands

Phenylquinazoline derivatives can also easily coordinate to the Pt(II) metal center.[37,49] Chang and coworkers have designed complexes **75** and **76** based on 4-phenylquinazoline with 2-pyridyl hexafluoropropoxide ancillary ligands (Figure 14). These complexes are characterized by intense orange emission with ^{3}MLCT character in DCM solution at room temperature, whereas pyridine analogues **75a** and **76a** are almost non-emissive in the same condition.[49] Both complexes are also luminescent in thin film without formation of excimers and/or aggregates. Complexes **77**–**80** are analogues of pyrimidine complexes **23**–**26**. Complexes **74** and **75** exhibit red-shifted emission with regards to pyrimidine analogues **23**–**24** (~100 nm) due to the stronger electron-deficient character of quinazoline (Tables 6 and 8).[50,51] Complex **77** exhibits even more bathochromically shifted emission than phenylpyrazine analogue **67** (~40 nm) (Figure 15). The solid-state emission of complexes **77** and **78** have a red shift up to 50 nm relative to emission in solution. The structureless, broad red-shifted emission can be explained by excimer formation in the solid state. Complexes **79** and **80** with diphenylamino ligands are non-emissive in solution, once again due to too strong charge transfer. Complexes **77** (λ_{em} = 728 nm, PLQY = 3%) **78** (λ_{em} =

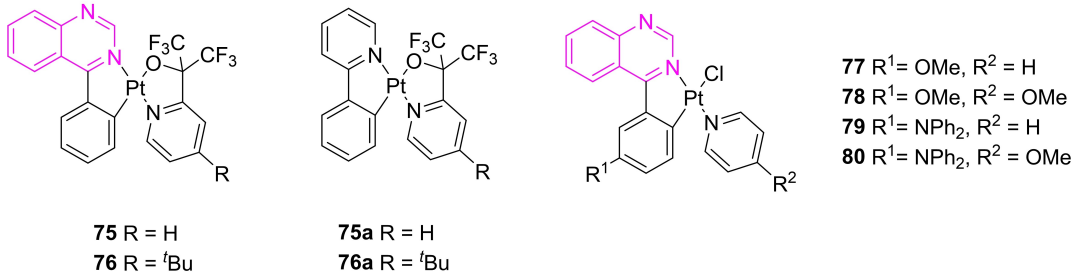

Figure 14. Cyclometalated complexes **75**–**80** with NC ligands containing quinazoline unit and pyridine analogues **75a** and **76a**.

Table 8. Photophysical properties of Pt(II) complexes **75**–**80** in degassed DCM solution at RT.

Pt(II) complex	Absorption λ_{max} (nm) ($\varepsilon\times10^{-3}$ M^{-1} cm^{-1})	Emission λ_{max} (nm)	PLQY (%)	τ (ns)	Ref.
75	292 (16), 347 (11), 364 (10), 400 (6.3), 481 (2.9)	595	47	2600	[47]
75a	291 (12), 351 (9.4), 405 (1.8)	499, 524	0.3	15.7	[47]
76	292 (16), 347 (11), 364 (10), 402 (6.9), 483 (3.1)	599	29	2600	[47]
76a	291 (14), 349 (11), 405 (2.0)	499, 525	0.5	33.7	[47]
77	274 (29.4), 351 (10.5), 401 (4.53), 504 (3.32)	671	26	5400	[37]
78	276 (22.4), 351 (8.05), 367 (7.53), 408 (3.98), 511 (3.13)	677	16	5100	[37]
79	280 (48.9), 299 (49.8), 345 (24.8), 364 (16.0), 397 (6.71), 546 (2.79), 563 (3.17)	–[a]	–[a]	–[a]	[37]
80	292 (38.9), 364 (12.9), 396 (6.44), 566 (3.23)	–[a]	–[a]	–[a]	[37]

[a] Emission too low to permit accurate measurement.

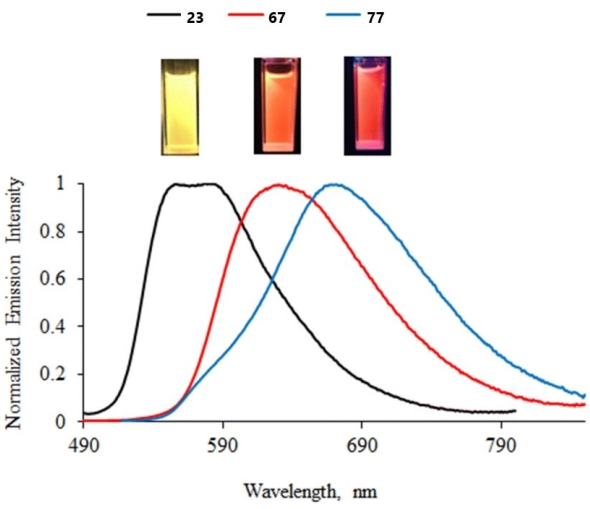

Figure 15. Normalized emission spectra of methoxy-substituted complexes **23**, **67**, **77** in deoxygenated DCM solution ($C \sim 10^{-5}$ M), Inset: picture of the DCM solutions taken under UV irradiation (from left to right **23**, **67** and **77**). Reproduced from Ref. [37] with permission from Royal Society of Chemistry.

720 nm, PLQY = 63 %) and **79** (λ_{em} = 795 nm, PLQY < 1 %) are characterized by NIR emission in solid state.

3.5. Quinoxaline Based Ligands

Only few Pt(II) complexes based on NC quinoxaline ligands are described in the literature (Figure 16).[39] Structural properties similar to those described above are observed: the annellation of pyrazine (**81** and **82** *vs* **72** and **74**) induces a bathochromic shift (> 90 nm), which is observed when comparing with the pyrimidine and quinazoline analogues. The complexation to a second Pt atom (**82** *vs* **81**) induces also a red-shifted emission due to stabilization of the LUMO (Figure 17, Table 9).

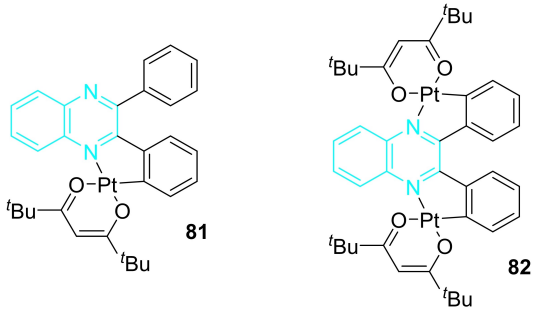

Figure 16. Complexes **81** and **82** with NC ligands containing quinoxaline unit.

4. Complexes with Tridentate NNN Diazine-Based Ligands

A change in the denticity of the ligand from 2 to 3 leads to the formation of a more rigid complex. The more planar and rigid nature of conjugated tridentate N-donor ligands, compared to bidentate ligands, can suppress the non-radiative decay pathway via molecular distortion, thereby improving the luminescence properties of NNN tridentate Pt(II) complexes. Indeed, this allows in particular to reduce the square planar→tetrahedral deformation upon photoexcitation. Furthermore, in tridentate complexes, the occurrence of unnecessary reductive elimination due to cis-coordinating monodentate ligands is avoided.

Only few complexes with NNN diazine-based ligands displaying emission properties are described in the literature. Zhang and coworkers have designed the series of neutral 2,6-(dipyridin-2-yl)pyrimidin-4(1*H*)-one Pt(II) complexes **83**–**85** (Figure 18).[52] These complexes, that exhibit rather high PLQY (Table 10) with ^{3}MLCT excited state, show reversible acid sensitivity caused by the protonation/deprotonation of the carbonyl oxygen. Nevertheless, platinum monochloride complex **83** exhibits lower PLQY and blue-shifted emission with regards to pyridinone analogue **83a**. Few cationic 2,4-(dipyridin-2-yl)pyrimidine Pt(II) complexes have been described but they do not exhibit any luminescent properties.[53]

5. Cyclometalated Complexes with Tridentate CNN Diazine Ligands

Cyclometalated Pt(II) complexes have generally better emission properties compared to NNN systems. The Pt–C bond, which acts as a very strong σ-donor and provides to the metal a very strong ligand field, induces an increase of the energy of high-lying non-radiative d-d states in comparison with NNN systems leading to better emission properties.[54] Cyclometalated CNN Pt(II) complexes can nevertheless exhibit struc-

Table 9. Photophysical properties of Pt(II) complexes **81** and **82** in degassed DCM solution.

Pt(II) complex	Absorption λ_{max} (nm) ($\varepsilon \times 10^{-3}$ M^{-1} cm^{-1})	Emission λ_{max} (nm)	PLQY (%)	τ (ns)	Ref.
81	294 (20.0), 373sh (9.38), 388 (1.6), 445 (6.47), 488sh (3.79)	668	14	3700	[39]
82	313 (21.6), 387 (14.2), 428 (8.16), 496 (1.36)	749	> 2.5	910	[39]

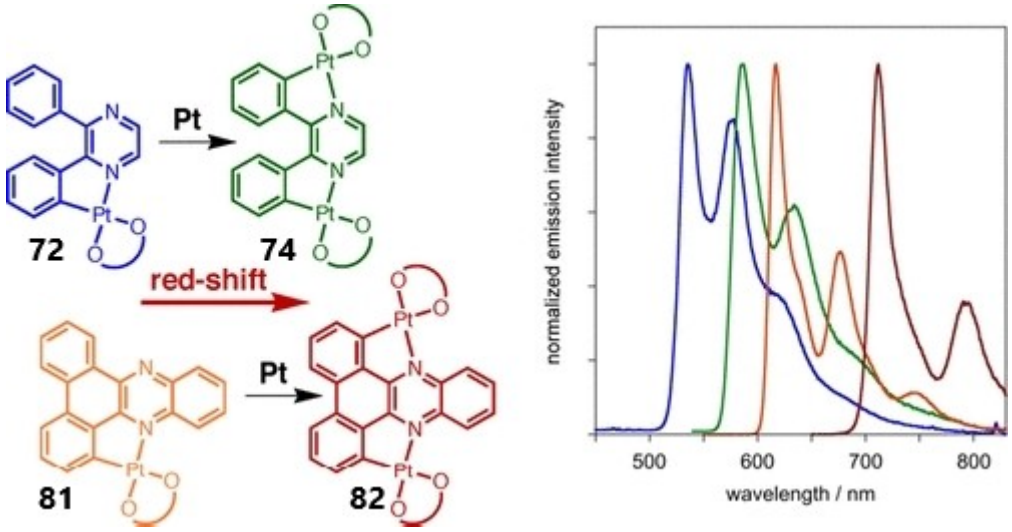

Figure 17. Normalized emission spectra of complexes **72**, **71**, **81** and **82** in degassed DCM. Adapted from Ref. [39] with permission from American Chemical Society.

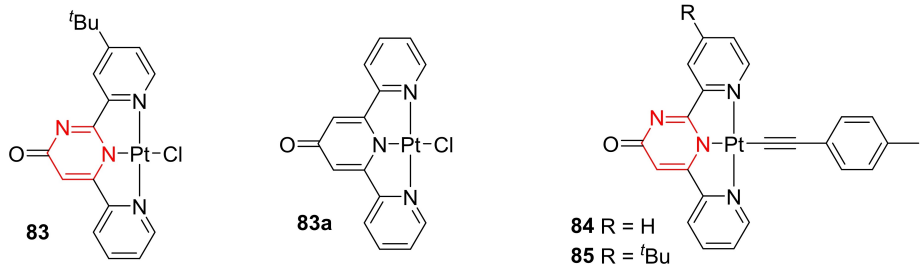

Figure 18. Structure of complexes **83**–**85** based on NNN 2,6-(dipyridin-2-yl)pyrimidin-4(1*H*)-one ligands and pyridinone analogue **83 a**.

Table 10. Photophysical properties of Pt(II) complexes **80**–**82** in degassed MeCN solution.

Pt(II) complex	Absorption λ_{max} (nm) ($\varepsilon \times 10^{-3}$ M^{-1} cm^{-1})	Emission λ_{max} (nm)	PLQY (%)	τ (ns)	Ref.
83	282 (16.8), 353 (4.12), 405 (5.79)	556	46	–[a]	[52]
83 a	285 (21.8), 310 (13.8), 324 (15.1), 445 (6.24)	585	100	1200	[52]
84	267 (48.8), 430 (8.50)	564	37	960	[52]
85	267 (40.5), 423 (7.40)	563	21	1300	[52]

[a] Not measured.

tural distortion in both singlet and, especially, triplet states,[55] as reflected in the Huang–Rhys factor (S_M). Appropriate structural modification of the tridentate ligand, along with a wise selection of ancillary ligands and incorporation with another metal center, can overcome this issue, resulting in the achievement of high PLQY.

Zhang and coworkers have performed a theoretical study on Pt(II) complex **86** based on various CNN complexes with phenylacetylene ancillary ligand.[56] Slightly red-shifted phosphorescence and increased radiative constant is predicted for complex **86** when compared to the pyridin-2-yl analogue **86 a** (Figure 19).

In our group, we have designed the complexes **87**–**96** based on phenyl,pyridin-2-ylpyrimidine ligands (Figure 20).[57] Except *N*,*N*-dimethylamino substituted complex **91**, all complexes exhibit yellow-to-red luminescence at room-temperature in diluted solution (Table 11). Compared to pyridine analogue **87 a**,[58] the chloro-platinum complexes **87** and **89** exhibit red-shifted emission. Compared to EDG, EWG on the alkynyl ancillary ligand induce a bathochromic shift of the

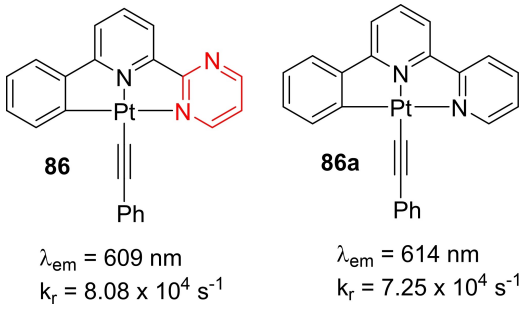

Figure 19. Structure of complexes **86** and **86a** and their theoretically predicted photophysical properties.

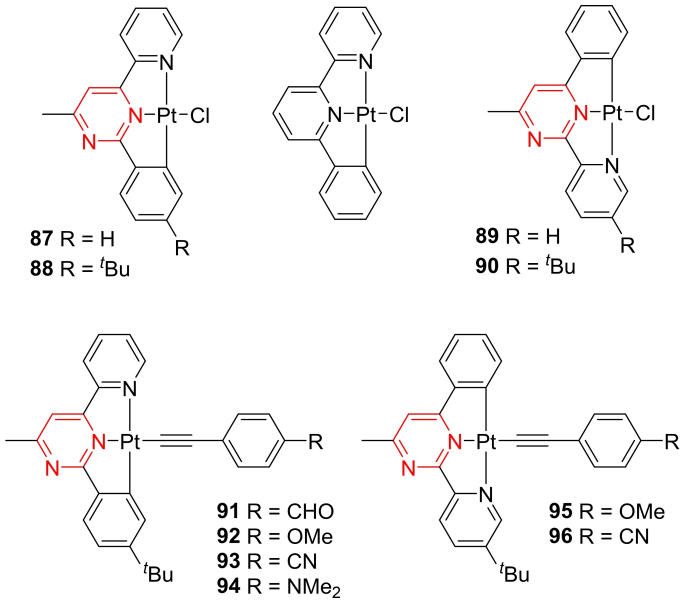

Figure 20. Structure of cyclometalated complexes **87**–**96** with CNN ligands containing pyrimidine unit and pyridine analogue **87a**.

emission band with increased emission intensity (**93** and **96** *vs* **92** and **95** respectively). The emission is also sensitive to the position of the pyridin-2-yl fragment on the pyrimidine core: when located in position 4 a redshift of emission is observed (**89**, **90**, **95** and **96** *vs* **87**, **88**, **92**, **93** respectively). In solid state, chloro-platinum complexes **87** and **89** without ^{t}Bu bulky group exhibit red-shifted excimer emission (Figure 21).

Wu and coworkers have designed a series of Ru–Pt heterobimetallic complexes **97**–**101** based on 2,3-di(2-pyridyl)-5,6-diphenylpyrazine and 2,3-di(2-pyridyl)-5-phenylpyrazine ligands (Figure 22).[59,60] Complexes **98**, **100** and **101** exhibit NIR emission contrary to complex **97** due to the absence of free-rotating phenyl groups on the pyrazine core (Table 12). Complexes **98** and **100** exhibit higher PLQY than that of the corresponding mono-Ru complex without Pt(II) due to mixed MLCT transitions from both the ruthenium and the platinum centers and an efficient energy transfer from the Ru(bpy)$_2$ moiety to the Pt component.[59] The NMe$_2$ containing complex **99** is not emissive in its neutral form due to low lying LLCT and reductive electron transfer from the NMe$_2$ group, but exhibits NIR emission upon gradual protonation.

6. Cyclometalated Complexes with Tridentate NCN Diazine Ligands

The rigidity and planarity of Pt(II) complexes have a positive impact on PLQY by reducing the non-radiative decays. CNN coordinated platinum(II) complexes can suffer from low PLQY due to the structural distortion, as observed in the previous chapter. A simple and efficient way to improve the photoluminescence efficiency of the complexes is to change the order of coordinating atoms around the Pt(II) metal center. NCN complexes show a smaller deviation from the planarity compared to CNN complexes. The NCN complexes have a shorter Pt–C (~1.90 Å) bond of the central phenyl ring than the isoelectronic tridentate CNN complexes (~2.04 Å),[1] resulting in a likely stronger σ-donor character of NCN ligands. Due to the shorter Pt–C bond, the bite angle of NCN complexes is more ideal compared to that of CNN complexes. A shorter Pt–C bond has a stronger interaction with the metal that allows to raise the non-radiative d-d state energetically higher than the emissive excited state. Moreover, NCN complexes suffer less from structural distortion in the ground and excited states than CNN complexes.[61] Synergetic effect of planarity, rigidity and strong ligand-field character of the σ-donor Pt–C bond enables the NCN complexes to achieve high PLQY. Similarly to CNN cyclometalated complexes, the photophysical data of NCN complexes can be modified by changing the design of the tridentate ligands and replacing the halogen with different types of ancillary ligands.

Cyclometalating 1,3-dipyrimidin-2-ylbenzene ligands have been used for complexation of Pt(II) (Figure 23).[62,63,64,65,66,67] Compared to its pyridine analogue **102a**, the complex **102** exhibits slightly blue shifted (6 nm) emission in DCM solution with reduced PLQY (32% instead of 60%) (Table 13). The presence of methoxy EDG in the central benzene core of the ligand (complex **103**) induces a red shift of the emission band with a slightly increased PLQY (Figure 24).[63] This complex exhibits red-shifted emission with higher PLQY than its pyridine analogue **103a**. On the other hand, the trifluoromethyl EWG in the structure of **104** is associated with a slight blue shift of the emission band as well as a significant reduction of PLQY.[63] In contrast to complex **103**, the flexible alkoxy chains in the structure of complex **105** and **106** enable solution processable self-assembly which induces Pt···Pt interaction allowing modulation of luminescence from

Table 11. Photophysical properties of Pt(II) complexes **84**–**93** in degassed DCM solution at RT.

Pt(II) complex	Absorption λ_{max} (nm) ($\varepsilon \times 10^{-3}$ $M^{-1}cm^{-1}$)	Emission λ_{max} (nm)	PLQY (%)	τ (ns)	Ref.
87	276 (21.8), 328 (7.0), 385 (3.6), 458 (2.6)	608	1.2	17 (86%), 301 (14%)	[57]
87a	278 (19.6), 325 (9.5), 360 (5.0), 430 (1.5), 510 (0.2)	565	–[a]	510	[58]
88	279 (26.1), 294sh (22.4), 339 (7.4), 387 (4.5), 458 (2.7)	608	1.4	21 (90%), 167 (10%)	[57]
89	266 (20.4) 291 (17.9), 321 (11.1), 390 (5.3)	544, 580	2.1	47	[57]
90	266 (16.4), 299 (15.3), 328sh (9.9), 386 (4.2)	551, 585	1.8	47	[57]
91	285 (24.3), 337 (21.2), 382sh (9.4), 464 (4.7)	628	2.1	70	[57]
92	282 (37.6), 345 (7.4), 388 (7.2), 483 (4.8)	655	0.9	–[a]	[57]
93	281 (59.5), 380 (6.2), 462 (3.6)	617	2.3	60	[57]
94	293 (59.5), 394 (5.6), 494 (3.5)	–[a]	–[a]	–[a]	[57]
95	270 (32.3), 294sh (25.2), 311sh (18.9), 332sh (11.7), 394 (7.4), 464 (4.0)	609	1.0	–[a]	[57]
96	265 (30.8), 280 (33.6), 311 (51.3), 391 (13.7), 422sh (10.7), 449sh (7.0)	582	5.5	160	[57]

[a] No measurement.

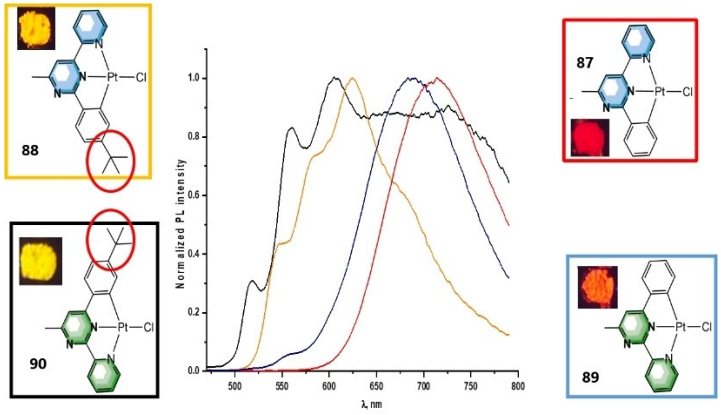

Figure 21. Normalized emission spectra of complexes **87**–**90** in solid state (powder) inset: picture of powder taken under UV irradiation.

Table 12. Photophysical properties of Ru–Pt heterobimetallic complexes **97**–**101** in degassed MeCN solution.

Pt(II) complex	Absorption λ_{max} (nm) ($\varepsilon \times 10^{-3}$ $M^{-1}cm^{-1}$)	Emission λ_{max} (nm)	PLQY (%)	τ (ns)	Ref.
97	274 (82), 315 (65), 372 (32), 394 (33), 561 (40)	–[a]	–[a]	–[a]	[59]
98	286 (78), 380 (30), 436 (20), 477 (20), 545 (20)	780	0.15	120	[59]
99	188 (83), 370 (22), 390 (22), 478 (17), 539 (14), 675 (9)	–[a]	–[a]	–[a]	[59]
100	286 (91), 380 (26), 432 (18), 480 (17), 550 (15)	784	0.14	–[a]	[59]
101	282 (95), 363 (33), 426 (22), 468 (22), 534 (24)	752	0.41	170	[60]

[a] Emission too low to permit accurate measurement.

visible to NIR.[65,66] Salthouse and coworkers have designed complexes **107**–**109** that differ by the nature of monodentate ancillary ligand (Figure 21).[67] Only minor difference in term of energy of Pt···Pt excimers are observed for these complexes in solution (Table 13), but in thin film significant differences are observed : for complex **109** with iodo ancillary ligand, aggregation is limited to the formation of dimer while for complex **108** with SCN– larger aggregate are observed leading to emission >850 nm. Whereas NIR-emitting OLED using complex **107** as emitter with =817 nm and EQE=1.2% was described,[62] with thiocyanate complex **108**, the device exhibits more bathochromically shifted emission with =944 nm and

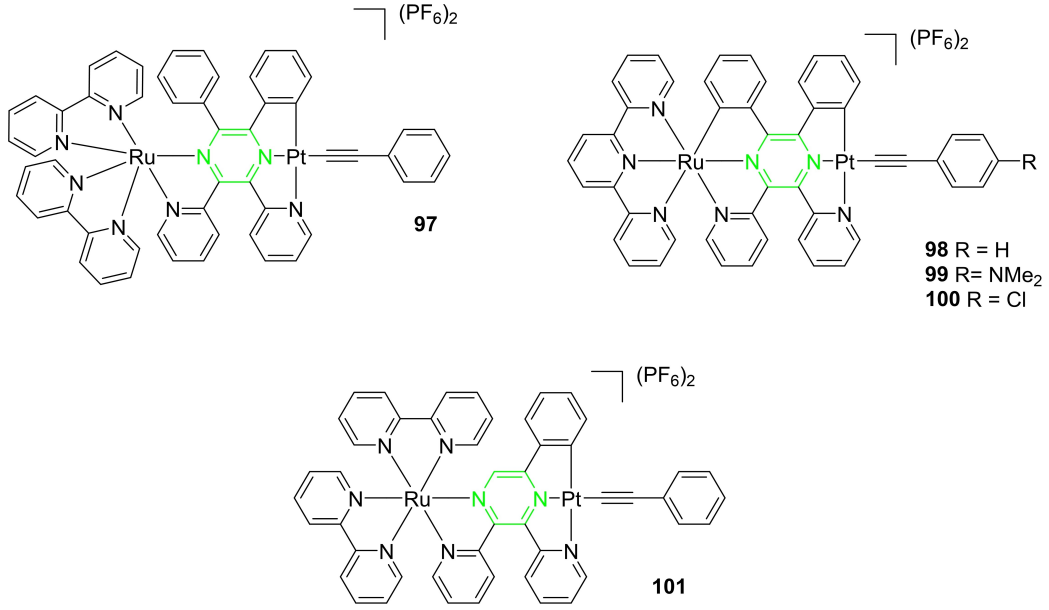

Figure 22. Structure of Ru–Pt heterobimetallic complexes **97–101** with CNN ligands containing pyrazine fragment.

Table 13. Photophysical properties of Pt(II) complexes **102–104, 102 a, 103 a, 107–120** in degassed DCM solution at RT.

Pt(II) complex	Absorption λ_{max} (nm) ($\varepsilon \times 10^{-3}$ M^{-1} cm^{-1})	Emission λ_{max} (nm)	PLQY (%)	τ (ns)	Ref.
102	267 (41.8), 382 (10.6), 408 (8.6), 479 (0.17)	484	32	5700	[59]
102 a	255 (25.2), 289 (21.1), 319 (6.1), 375 (8.6), 402 (7.0), 452 (0.15), 485 (0.14)	490	60	7200	[59]
103	267 (23.3), 363 (2.1), 381 (3.3), 448 (4.9)	561, 589	37	9500	[63]
103 a	282 (25.0), 293 (27.6), 363 (4.3), 375 (6.3), 440 (8.6), 510 (0.08)	547	30	13000	[59]
104	263 (28.1), 363 (5.0), 379 (7.4), 404 (5.5)	476, 508, 549	8	5600	[63]
107	270 (22.1), 362sh (2.55), 387 (4.83), 40 (4.48)	500, 531, 584sh, 701	60	7900	[67]
108	266 (35.5), 279 (29.0), 359 (4.12), 388 (7.40), 400 (7.18), 417 (7.08)	497, 659	67	8400	[67]
109	279 (23.1), 400 (4.98), 420 (5.01)	502, 709	81	6600	[67]
110	270 (44.9), 315 (10.5), 393 (6.6), 426 (4.9)	507, 524	7	5000	[63]
111	269 (35.3), 322 (7.1), 445 (2.4)	538	27	6700	[63]
112	274 (23.1), 307 (18.6), 390 (2.2), 422 (1.3)	498, 522	16	5600	[63]
113	268 (22.4), 382 (2.1), 451 (3.5)	562, 593	55	9100	[63]
114	69 (86.0), 381 (7.4), 458 (11.3)	572, 590	81	9100	[63]
115	274 (49.0), 306 (42.0), 392 (9.5), 450 (11.9)	561	35	7100	[63]
116	269 (27.1), 336 (4.4), 381 (2.3), 448 (3.2)	561, 592	52	12300	[63]
117	272 (59.9), 317 (51.0), 381 (13.6), 457 (13.8)	605	1	–[a]	[63]
118	265 (38.9), 315 (7.6), 393 (6.6), 425 (5.3)	506	6	3400	[63]
119	266 (30.1), 318 (3.9), 380 (1.5), 445 (1.9)	552	18	4300	[63]
120	272 (29.6), 305 (25.8), 373 (6.6), 389 (7.6), 418 (6.1)	495	2	3100	[63]

[a] Emission too low to permit accurate measurement.

EQE = 0.3 %.[67] The presence of alkynyl ancillary ligand in the structure of complexes **110–120**, has a limited influence on absorption and emission spectra except in case of complex **117** with strong NPh_2 EDG for which a significant red shift is observed (Table 13).[63] The presence of two methoxy substituents on both the 1,3-bis(pyrimidin-2yl)benzene ligand and the alkynyl ancillary ligand (complex **114**) has a beneficial effect on PLQY (81 %), one of the best ever reported for this class of complexes.

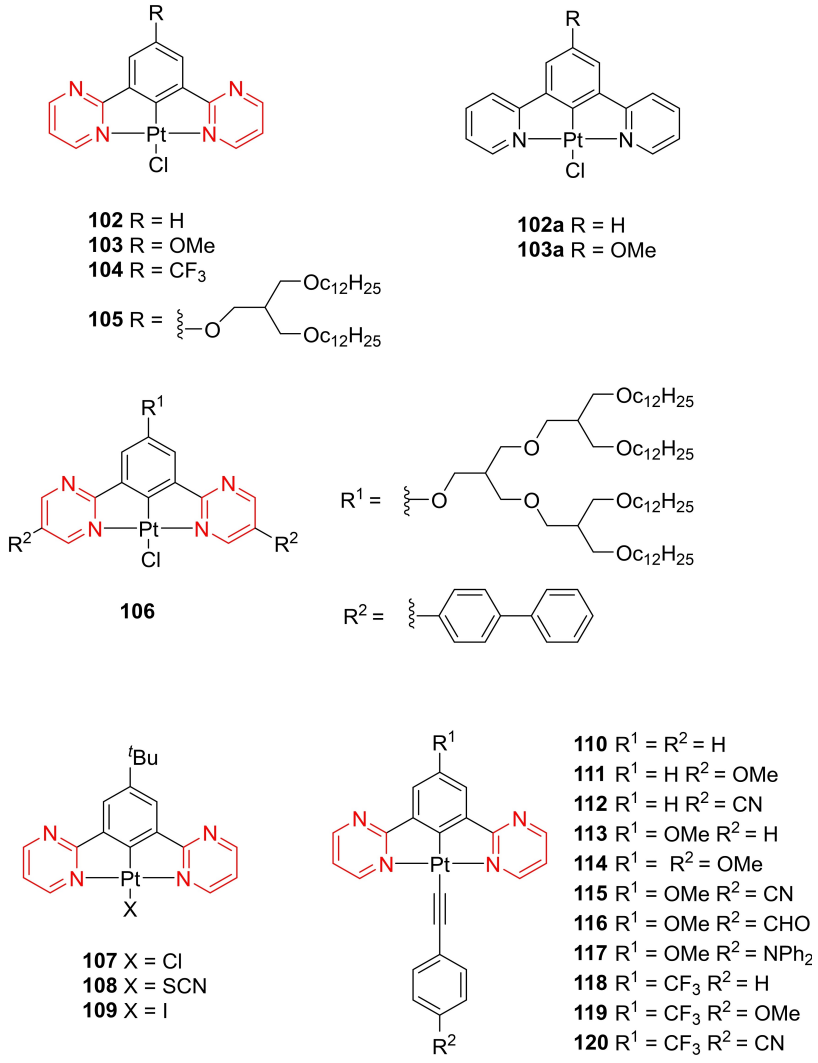

Figure 23. Structure of cyclometalated Pt(II) complexes **102–120** with NCN ligands containing pyrimidine fragments and puridine analogues **102a** et **102b**.

7. Cyclometalated Complexes with Tetradentate NCNO Diazine-Based Ligands

The study of phosphorescent platinum complexes based on tetradentate cyclometalating ligands is a rapidly developing field, but already represents important progress in the search for highly efficient and robust triplet emitters for application in OLED devices. To be best of our knowledge, only one Pt(II) complex with diazine-based ligand of this type has been described in the literature so far.

Pander and coworkers have designed dinuclear Pt(II) complex **121** with NCNO ligand (Figure 25).[68] This complex is characterized by an extremely high rigidity and a small singlet-triplet energy difference ($\Delta E_{ST} = 69$ meV). It exhibits thermally activated delayed fluorescence (TADF) instead of phosphorescence, which is rather unique for Pt(II) complexes. Complex **118** was incorporated into solution-processed OLEDs displaying red emission ($\lambda_{EL} = 607$ nm) achieving $EQE_{max} = 7.4\,\%$.

8. Conclusion

In summary, around one hundred diazine based Pt(II) complexes have been described in the literature for their luminescence properties. Most of them are cyclometalated complexes with NC, NCN or NNC pyrimidine ligands. Pyrimidine complexes are often characterized by red-shifted emission and sometimes higher PLQY compared to pyridine analogues. Due to the presence of two nitrogen lone pairs, diazines have the ability to coordinate simultaneously to two similar or different metal centers, which allows tune the energy and intensity of emission. Generally, this induces red-shifted

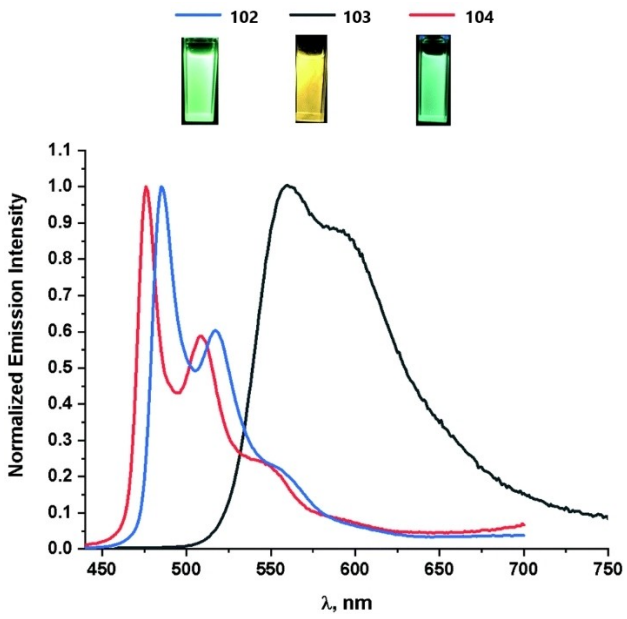

Figure 24. Normalized emission spectra of chloro-platinum complexes **102**–**104** in deoxygenated CH_2Cl_2 solution ($c \sim 10^{-5}$ M). λ_{exc} = of the lowest energy band; inset: picture of CH_2Cl_2 solution taken under UV irradiation. Reproduced from Ref. [63] with permission from Royal Society of Chemistry.

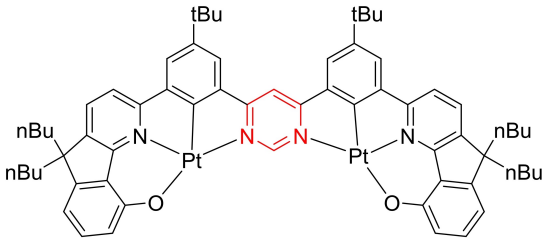

Figure 25. Structure of cyclometalated Pt(II) complex **121** with NCNO ligand containing pyrimidine unit.

emission and increased PLQY: some on such complexes exhibit NIR emission with almost no emission of visible light. Pyrazine complexes are rarer, and exhibit significantly red-shifted emission with regards to pyrimidine analogues due to the presence of the second nitrogen atom in conjugated position vs the Pt(II) center. Only few quinoxaline and quinazoline Pt(II) complexes are known in the literature, they are characterized by red-shifted emission with regards to their pyrimidine and pyrazine analogue because benzodiazine fragments exhibit a stronger electron-deficient character. Some of these complexes exhibit interesting NIR emission. Diazine based Pt(II) complexes have found application in doped and nondoped OLEDs, sometimes with higher performances than pyridine analogues. Red and NIR OLED based on diazine Pt(II) complexes are particularly attracting. Underexplored pyrazine, quinazoline and quinoxaline Pt(II) complexes should draw the attention of researcher in the near future in this context.

Acknowledgements

M. H. acknowledges the Région Bretagne, France and Conseil Départemental des Côtes d'Armor, France for her Ph.D. funding (MMLum project). Authors are grateful to the EUR LUMOMAT project and the Investments for the Future program ANR-18-EURE-0012.

References

[1] *Photochemistry and Photophysics of Coordination Compounds II*; Balzani, V., Campagna, S., Eds.; Topics in Current Chemistry; Springer Berlin Heidelberg: Berlin, Heidelberg, **2007**; Vol. 281.
[2] a) W. B. Connick, H. B. Gray, *J. Am. Chem. Soc.* **1997**, *119*, 11620–11627; b) C. N. Pettijohn, E. B. Jochnowitz, B. Chuong, J. K. Nagle, A. Vogler, *Coord. Chem. Rev.* **1998**, *171*, 85–92; c) W. B. Connick, D. Geiger, R. Eisenberg, *Inorg. Chem.* **1999**, *38*, 3264–3265; d) D. K. Crites Tears, D. R. McMillin, *Coord. Chem. Rev.* **2001**, *211*, 195–205.
[3] L. Chassot, A. von Zelewsky, D. Sandrini, M. Maestri, V. Balzani, *J. Am. Chem. Soc.* **1986**, *108*, 6084–6085.
[4] a) C. Murawski, K. Leo, M. C. Gather, *Adv. Mater.* **2013**, *25*, 6801–6827; b) J. D. Bullock, A. Salehi, C. J. Zeman, K. A. Abboud, F. So, K. S. Schanze, *ACS Appl. Mater. Interfaces* **2017**, *9*, 41111–41114.
[5] H. R. Shahsavari, S. Paziresh, *New J. Chem.* **2021**, *45*, 22732–22740.
[6] J. A. G. Williams, *Chem. Soc. Rev.* **2009**, *38*, 1783–1801.
[7] Y. Luo, Y. Xu, W. Zhang, W. Li, M. Li, R. He, W. Shen, *J. Phys. Chem. C* **2016**, *120*, 3462–3471.
[8] a) W. Lu, B.-X. Mi, M. C. W. Chan, Z. Hui, C.-M. Che, N. Zhu, S.-T. Lee, *J. Am. Chem. Soc.* **2004**, *126*, 4958–4971; b) T. Theiss, S. Buss, I. Maisuls, R. López-Arteaga, D. Brünik, J. Kösters, A. Hepp, N. L. Dolsinis, E. A. Weiss, C. A. Strassert, *J. Am. Chem. Soc.* **2023**, *145*, 3937–3951; c) M. Krause, J. Friedel, S. Buss, D. Brünink, A. Berger, C. A. Strassert, N. L. Dolsinis, A. Klein, *Dalton Trans.* **2022**, *51*, 16181–16194; d) B. Li, Y. Li, M. H.-Y. Chan, V. W.-W. Yam, *J. Am. Chem. Soc.* **2021**, *143*, 21676–21684; e) J. A. G. Williams, *Photochem. Photophys. Coord. Compds* **2007**, *281*, 205–268.
[9] a) Y.-C. Wei, K.-H. Kuo, Y. Chi, P.-T. Chou, *Acc. Chem. Res.* **2023**, *56*, 689–699; b) K. M.-C. Wong, V. W.-W. Yam, *Acc. Chem. Res.* **2011**, *44*, 424–434; c) M. A. Soto, R. Kandel, M. J. MacLachlan, *Eur. J. Inorg. Chem.* **2021**, 894–906.
[10] a) A. Haque, L. Xu, R. A. Al-Balushi, M. K. Al-Suti, R. Ilmi, Z. Guo, M. S. Khan, W.-Y. Wong, P. R. Raithby, *Chem. Soc. Rev.* **2019**, *48*, 5547–5563; b) C. Cebrian, M. Mauro, *Beilstein J. Org. Chem.* **2018**, *14*, 1459–1481; c) T. Strassner, *Acc. Chem. Res.* **2016**, *49*, 2680–2689; d) M.-C. Tang, A. K. W. Chan, M.-Y. Chan, V. W.-W. Yam, *Top. Curr. Chem.* **2016**, *374*, 46; e) S. Huo, J. Carroll, D. A. K. Vezzu, *Asian J. Org. Chem.*

2015, *4*, 1210–1424; f) J. Kalinnowski, V. Fattori, M. Cocchi, J. A. G. Williams, *Coord. Chem. Rev.* **2011**, *255*, 2401–2425.
[11] a) P.-K. Chow, G. Cheng, G. S. M. Tong, W.-P. To, W.-L. Kwong, K.-H. Low, C.-C. Kwok, C. Ma, C.-M. Che, *Angew. Chem. Int. Ed.* **2015**, *54*, 2084–2089; b) D. Saito, T. Ogawa, M. Yoshida, J. Takayama, S. Hiura, A. Murayama, A. Kobayashi, M. Kato, *Angew. Chem. Int. Ed.* **2020**, *59*, 18723–18730; c) J. Hu, M. Nikravesh, H. R. Shahsavari, R. Babadi Aghakhanpour, A. L. Rheingold, M. Alshami, Y. Sakamaki, H. A. Beyzavi, *Inorg. Chem.* **2020**, *59*, 16319–16327; d) X. Yang, L. Yue, Y. Yu, B. Liu, J. Dang, Y. Sun, G. Zhou, Z. Wu, W.-Y. Wong, *Adv. Opt. Mater.* **2020**, *8*, 2000079; e) M. Bachmann, D. Suter, O. Blacque, K. Venkatesan, *Inorg. Chem.* **2016**, *55*, 4733–4745; f) T. Fleetham, G. Li, J. Li, *Adv. Mater.* **2017**, *29*, 1601861; g) J. A. G. Williams, A. Beeby, E. S. Davies, J. A. Weinstein, C. Wilson, *Inorg. Chem.* **2003**, *42*, 8609–8611; h) M. Mydlak, M. Mauro, F. Polo, M. Felicetti, J. Leonhardt, G. Diener, L. De Cola, C. A. Strassert, *Chem. Mater.* **2011**, *23*, 3659–3667; i) A. Amar, H. Meghezzi, J. Boixel, H. le Bozec, V. Guerchais, D. Jacquemin, A. Boucekkine, *J. Phys. Chem. A* **2014**, *118*, 6278–6286.
[12] a) I. Haiduc, *J. Coord. Chem.* **2019**, *72*, 2805–2903; b) H. Araki, K. Tsuge, Y. Sasaki, S. Ishizaka, N. Kitamura, *Inorg. Chem.* **2005**, *44*, 9667–9675.
[13] a) M. Barboiu, G. Vaughan, N. Kyritsakas, J.-M. Lehn, *Chem. Eur. J.* **2003**, *9*, 763–769; b) P. J. Steel, C. M. Fitchett, *Coord. Chem. Rev.* **2008**, *252*, 990–1006; c) L. A. Cuccia, J.-M. Lehn, J.-C. Homo, M. Schmutz, *Angew. Chem. Int. Ed.* **2000**, *39*, 233–237.
[14] E. G. Brown, *Ring Nitrogen and Key Biomolecules: The Biochemistry of N-Heterocycles*; Kluwer academic Publishers: Dordrecht; Boston; London, **1998**.
[15] a) A. Vyas, B. Sahu, S. Pathania, N. K. Nandi, G. Chauhan, V. Asati, B. Kumar, *J. Heterocycl. Chem.* **2023**, *in press* 10.1002/jhet.4593; b) I. M. Lagoja, *Chem. Biodiversity* **2005**, *2*, 1–50.
[16] a) S. Achelle, J. Rodríguez-López, F. Robin-le Guen, *ChemistrySelect* **2018**, *3*, 1852–1886; b) S. Achelle, N. Plé, A. Turck, *RSC Adv.* **2011**, *1*, 364–388; c) S. Achelle, C. Baudequin, N. Plé, *Dyes Pigm.* **2013**, *98*, 575–600; d) S. Achelle, J. Rodríguez-López, F. Bureš, F. Robin-le Guen, *Chem. Rec.* **2020**, *20*, 440–451; e) M. Fecková, P. le Poul, Bureš, F. Robin-le Guen, S. Achelle, *Dyes Pigm.* **2020**, *182*, 108659; f) S. Achelle, M. Hodée, J. Massue, A. Fihey, C. Katan, *Dyes Pigm.* **2022**, *200*, 110157.
[17] a) G. Orellana, C. Alvarez Ibarra, J. Santoro, *Inorg. Chem.* **1988**, *27*, 1025–1030; b) K. Roussel, A. Cartier, A. Marsura, *Chem. Phys. Lett.* **2003**, *367*, 463–467.
[18] J. S. Doll, N. I. Regenauer, V. P. Bothe, H. Wadepohl, D.-A. Roşca, *Inorg. Chem.* **2022**, *61*, 520–532.
[19] M. U. Anwar, A. Al-Harrasi, E. L. Gavey, M. Pilkington, J. M. Rawson, L. K. A. Thompson, *Dalton Trans.* **2018**, *47*, 2511–2521.
[20] J. Zhao, J. Yuan, Z. Fang, S. Huang, Z. Chen, F. Qiu, C. Lu, J. Zhu, X. Zhuang, *Coord. Chem. Rev.* **2022**, *471*, 214735.
[21] a) S. Derossi, M. Casanova, E. Iengo, E. Zangrando, M. Stener, E. Alessio, *Inorg. Chem.* **2007**, *46*, 11243–11253; b) J. Suarez-Varela, A. J. Mota, H. Aouryaghal, J. Cano, A. Rodriguez-Dieguez, D. Luneau, E. Colacio, *Inorg. Chem.* **2008**, *47*, 8143–8458; c) K. V. Domasevitch, P. V. Solntsev, I. A. Gural'skiy, H. Krautsheid, E. B. Rusanov, A. N. Chernega, J. A. K. Howard, *Dalton Trans.* **2007**, *35*, 3893–3905.
[22] a) S. Zhang, J.-C. Xia, Z.-G. Wu, G.-Z. Lu, Y. Zhao, Y.-X. Zheng, *Eur. J. Inorg. Chem.* **2016**, *15–16*, 2556–2561; b) C. Hadad, S. Achelle, I. López-Solera, J. C. García-Martínez, J. Rodríguez-López, *Dyes Pigm.* **2013**, *97*, 230–237.
[23] D. Chen, S.-J. Su, Y. Cao, *J. Mater. Chem. C* **2014**, *2*, 9565–9578.
[24] M.-C. Tang, A. K.-W. Chan, M.-Y. Chan, V. W.-W. Yam, in *Photoluminescent Materials and Electroluminescent Devices* (Ed.: N. Armaroli, H. Bolink), Springer, **2016**, pp. 67–109.
[25] a) M. S. McCready, R. J. Puddephatt, *Organometallics* **2015**, *34*, 2261–2270; b) M. E. Moustafa, P. D. Boyle, R. J. Puddephatt, *Can. J. Chem.* **2014**, *92*, 706–715.
[26] P. Ganesan, W.-Y. Hung, J.-Y. Tso, C.-L. Ko, T.-H. Wang, P.-T. Chen, H.-F. Hsu, S.-H. Liu, G.-H. Lee, P.-T. Chou, A. K.-Y. Jen, Y. Chi, *Adv. Funct. Mater.* **2019**, *29*, 1900923.
[27] a) Q. Wang, I. W. H. Oswald, X. Yang, G. Zhou, H. Jia, Q. Qiao, Y. Chen, J. Hoshikawa-Halbert, B. E. Gnade, *Adv. Mater.* **2014**, *26*, 8107–8113; b) K.-H. Kim, J.-K. Liao, S. W. Lee, B. Sim, C.-K. Moon, G.-H. Lee, H. J. Kim, Y. Chi, J.-J. Kim, *Adv. Mater.* **2016**, *28*, 2526–2532; c) S.-Y. Chang, J. Kavitha, S.-W. Li, C.-S. Hsu, Y. Chi, Y.-S. Yeh, P.-T. Chou, G.-H. Lee, A. J. Carty, Y.-T. Tao, C.-H. Chien, *Inorg. Chem.* **2006**, *45*, 137–146.
[28] a) Q. Wang, I. W. H. Oswald, X. Yang, G. Zhou, H. Jia, Q. Qiao, Y. Chen, J. Hoshikawa-Halbert, B. E. Gnade, *Adv. Mater.* **2014**, *26*, 8107–8113; b) K.-H. Kim, J.-K. Liao, S. W. Lee, B. Sim, C.-K. Moon, G.-H. Lee, H. J. Kim, Y. Chi, J.-J. Kim, *Adv. Mater.* **2016**, *28*, 2526–2532; c) S.-Y. Chang, J. Kavitha, S.-W. Li, C.-S. Hsu, Y. Chi, Y.-S. Yeh, P.-T. Chou, G.-H. Lee, A. J. Carty, Y.-T. Tao, C.-H. Chien, *Inorg. Chem.* **2006**, *45*, 137–146.
[29] a) B. Blondel, F. Delarue, M. Lopes, S. Lodeira-Mallet, F. Alary, C. Renaud, I. Sasaki, *Synth. Met.* **2017**, *227*, 106–116; b) L. Brenda, B. Doistau, B. Hasenknopf, G. Vives, *Molecules* **2018**, *23*, 990; c) G. Cheng, S. C. F. Kui, W.-H. Ang, M.-Y. Ko, P.-K. Chow, C.-L. Kwong, C.-C. Kwok, C. Ma, X. Guan, K.-H. Low, S.-J. Su, C.-M. Che, *Chem. Sci.* **2014**, *5*, 4819–4830.
[30] J. A. G. Williams, *Top. Curr. Chem.* **2007**, *281*, 205–208.
[31] D. D. Zhukovsky, V. V. Sizov, G. L. Starova, S. P. Tunik, E. V. Grachova, *J. Organomet. Chem.* **2018**, *867*, 367–374.
[32] M. A. Zhukovskaya, D. D. Zhukovsky, V. V. Pavloskiiy, V. V. Porsev, R. A. Evarestov, S. P. Tunik, *Inorg. Chem. Commun.* **2018**, *98*, 105–110.
[33] Y. Sun, X. Yang, B. Liu, H. Guo, G. Zhou, W. Ma, Z. Wu, *J. Mater. Chem. C* **2019**, *7*, 12552–12559.
[34] G. Zhou, Q. Wang, X. Wang, C.-L. Ho, W.-Y. Wong, D. Ma, L. Wag, Z. Lin, *J. Mater. Chem.* **2010**, *20*, 7472–7484.
[35] J. Zhao, F. Dang, Z. Feng, B. Liu, X. Yang, Y. Wu, G. Zhou, Z. Wu, W.-Y. Wong, *Chem. Commun.* **2017**, *53*, 7581–7584.
[36] M. Fecková, S. Kahlal, T. Roisnel, J.-Y. Saillard, J. Boixel, M. Hruzd, P. le Poul, S. Gauthier, F. Robin-le Guen, F. Bureš, S. Achelle, *Eur. J. Inorg. Chem.* **2021**, 1592–1600.

[37] M. Hruzd, S. Kahlal, N. le Poul, L. Wojcik, M. Cordier, J.-Y. Saillard, J. Rodríguez-López, F. Robin-le Guen, S. Gauthier, S. Achelle, *Dalton Trans.* **2023**, *52*, 1927–1938.
[38] C. Damm, G. Israel, T. Hegmann, C. Tschierske, *J. Mater. Chem.* **2006**, *16*, 1808–1816.
[39] S. Culham, P.-H. Lanoë, V. L. Whittle, M. C. Durrant, J. A. G. Williams, V. N. Kozhevnikov, *Inorg. Chem.* **2013**, *52*, 10992–11003.
[40] V. N. Kozhevnikov, M. C. Durrant, J. A. G. Williams, *Inorg. Chem.* **2011**, *50*, 6304–6313.
[41] M. Z. Shafikov, R. Daniels, P. Pander, F. B. Dias, J. A. G. Williams, V. N. Kozhevnikov, *ACS Appl. Mater. Interfaces* **2019**, *11*, 8182–8193.
[42] M. Z. Shafikov, P. Pander, A. V. Zaytsev, R. Daniels, R. Martinscoft, F. B. Dias, J. A. G. Williams, V. N. Kozhevnikov, *J. Mater. Chem. C* **2021**, *9*, 127–135.
[43] Y. Sun, B. Liu, Y. Guo, X. Chen, Y.-Y. Lee, Z. Feng, C. Adachi, G. Zhou, Z. Chen, X. Yang, *ACS Appl. Mater. Interfaces* **2021**, *13*, 36020–36032.
[44] M. Z. Shafikov, S. Tang, C. Larsen, M. Bodensteiner, V. N. Kozhevnikov, L. Edman, *J. Mater. Chem. C* **2019**, *7*, 10672–10682.
[45] S. F. Wang, Y. Yuan, Y.-C. Wei, W.-H. Chan, L.-W. Fu, B.-K. Su, I. Y. Chen, K.-J. Chou, P.-T. Chen, H.-F. Hsu, C.-L. Ko, W.-Y. Hung, C.-S. Lee, P.-T. Chou, Y. Chi, *Adv. Funct. Mater.* **2020**, *30*, 2002173.
[46] Y.-C. Wei, S. F. Wang, Y. Hu, L.-S. Liao, D.-G. Chen, K.-H. Chang, C.-W. Wang, S.-H. Liu, W.-H. Chan, J.-L. Liao, W.-Y. Hung, T.-H. Wang, P.-T. Chen, H.-F. Hsu, Y. Chi, P.-T. Chou, *Nat. Photonics* **2020**, *14*, 570–577.
[47] S. F. Wang, L.-W. Fu, Y.-C. Wei, S.-H. Liu, J.-A. Lin, G.-H. Lee, P.-T. Chou, J.-Z. Huang, C.-I. Wu, Y. Yuan, C.-S. Lee, Y. Chi, *Inorg. Chem.* **2019**, *58*, 13892–13901.
[48] P. Pander, G. Turnbull, A. V. Zaytsev, F. B. Dias, V. N. Kozhevnikov, *Dyes Pigm.* **2021**, *184*, 108857.
[49] S.-Y. Chang, Y.-M. Cheng, Y. Chi, Y.-C. Lin, C.-M. Jiang, C.-M. Jiang, G.-H. Lee, P.-T. Chou, *Dalton Trans.* **2008**, 6901–6911.
[50] S. Achelle, F. Robin-le Guen, *J. Photochem. Photobiol. A* **2017**, *348*, 281–286.
[51] S. Achelle, J. Rodríguez-López, F. Robin-le Guen, *J. Org. Chem.* **2014**, *79*, 7564–7571.
[52] H. Zhang, B. Zhang, Y. Li, W. Sun, *Inorg. Chem.* **2009**, *48*, 3617–3627.
[53] E. Morel, C. Beauvineau, D. Naud-Martin, C. Landras-Guetta, D. Verga, D. Ghosh, S. Achelle, F. Mahuteau-Betzer, S. Bombard, M.-P. Teulade-Fichou, *Molecules* **2019**, *21*, 404.
[54] A. Haque, L. Xu, R. A. Al-Balushi, M. K. Al-Suti, R. Ilmi, Z. Guo, M. S. Khan, W.-Y. Wong, P. R. Raithby, *Chem. Soc. Rev.* **2019**, *48*, 5547–5563.
[55] P.-K. Chow, G. Cheng, G. S. M. Tong, W.-P. To, W.-L. Kwong, K.-H. Low, C.-C. Kwok, C. Ma, C.-M. Che, *Angew. Chem. Int. Ed.* **2015**, *54*, 2084–2089.
[56] W. Zhang, J. Wang, Y. Xu, W. Li, W. Shen, *J. Organomet. Chem.* **2017**, *836–837*, 26–33.
[57] M. Hruzd, S. Gauthier, J. Boixel, S. Kahlal, N. le Poul, J.-Y. Saillard, S. Achelle, F. Robin-le Guen, *Dyes Pigm.* **2021**, *194*, 109622.
[58] S.-W. Lai, M. C.-W. Chang, T.-C. Cheung, S.-M. Peng, C.-M. Che, *Inorg. Chem.* **1999**, *38*, 4046–4055.
[59] S.-H. Wu, S. E. Burkhardt, J. Yao, Y.-W. Zhong, H. D. Abruña, *Inorg. Chem.* **2011**, *50*, 3959–3969.
[60] S.-H. Wu, Y.-W. Zhong, J. Yao, *Chem. Asian J.* **2013**, *8*, 1504–1513.
[61] W. Shen, W. Zhang, C. Zhu, *Phys. Chem. Chem. Phys.* **2017**, *19*, 23532–23540.
[62] Z. Wang, E. Turner, V. Mahoney, S. Madakuni, T. Groy, J. Li, *Inorg. Chem.* **2010**, *49*, 11276–11286.
[63] M. Hruzd, N. le Poul, M. Cordier, S. Kahlal, J.-Y. Saillard, S. Achelle, S. Gauthier, F. Robin-le Guen, *Dalton Trans.* **2022**, *51*, 5546–5560.
[64] X. Li, J. Hu, Y. Wu, R. Li, D. Xias, W. Zheng, D. Zhang, Y. Xiang, W. Jin, *Dyes Pigm.* **2017**, *141*, 188–194.
[65] L. Yang, J. Hu, W. Zheng, Y. Wu, X. Li, D. Zhang, W. Jin, *Chin. J. Org. Chem.* **2017**, *37*, 2647–2654.
[66] P. Pander, A. Sil, R. J. Salthouse, C. W. Harris, M. T. Walden, D. S. Yufit, J. A. G. Williams, F. B. Dias, *J. Mater. Chem. C* **2022**, *10*, 15084–15095.
[67] R. J. Salthouse, P. Pander, D. S. Yufit, F. B. Dias, J. A. G. Williams, *Chem. Sci.* **2022**, *13*, 13600–13610.
[68] P. Pander, R. Daniels, A. V. Zaytsev, A. Horn, A. Sil, T. J. Penfold, J. A. G. Williams, V. N. Kozhevnikov, F. B. Dias, *Chem. Sci.* **2021**, *12*, 6172–6180.

Manuscript received: October 31, 2023
Revised manuscript received: March 18, 2024
Version of record online: ■■ ■■, ■■■■

REVIEW

This review summarizes the results of the litterature regarding the photophisical properties of platinum (II) complexes with diazine-based ligands. Results are compared to pyridine analogues. The device performances of complexes used as emitters in OLEDs are also discussed.

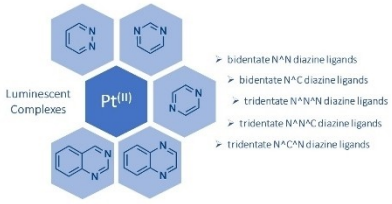

*M. Hruzd, R. Durand, S. Gauthier, P. le Poul, F. Robin-le Guen, S. Achelle**

1 – 24

Photoluminescence of Platinum(II) Complexes with Diazine-Based Ligands